

Error matrices in quantum process tomography

Alexander N. Korotkov

Department of Electrical Engineering, University of California, Riverside, California 92521

(Dated: November 6, 2013)

We discuss characterization of experimental quantum gates by the error matrix, which is similar to the standard process matrix χ in the Pauli basis, except the desired unitary operation is factored out, by formally placing it either before or after the error process. The error matrix has only one large element, which is equal to the process fidelity, while other elements are small and indicate imperfections. The imaginary parts of the elements along the left column and/or top row directly indicate the unitary imperfection and can be used to find the needed correction. We discuss a relatively simple way to calculate the error matrix for a composition of quantum gates. Similarly, it is rather straightforward to find the first-order contribution to the error matrix due to the Lindblad-form decoherence. We also discuss a way to identify and subtract the tomography procedure errors due to imperfect state preparation and measurement. In appendices we consider several simple examples of the process tomography and also discuss an intuitive physical interpretation of the Lindblad-form decoherence.

PACS numbers: 03.65.Wj, 03.65.Yz, 03.67.-a, 85.25.Cp

I. INTRODUCTION

Quantum process tomography (QPT) [1–9] is a way to completely characterize a quantum process. It is the main tool for experimental characterization of quantum gates, being developed for potential use in a quantum computer. QPT has been realized in numerous experiments, practically in all types of qubit systems, including, e.g., NMR [10, 11], linear optics [6, 12, 13], ion traps [14, 15], and superconducting qubits [16–21]. In this paper we mainly focus on QPT with superconducting qubits, even though our discussion is applicable to other systems as well.

Unfortunately, QPT requires resources, which scale exponentially with the number of qubits. For N (superconducting) qubits the number of initial states is usually 4^N (or sometimes 6^N), and the number of “measurement directions” (state tomography “rotations”) for each initial state is typically 3^N (or 6^N). Each such setup typically requires a few hundred or a few thousand experimental runs. From this scaling it is easy to estimate that the QPT of a 1-qubit or a 2-qubit quantum gate requires a manageable number of experimental runs, while a 3-qubit QPT is rather difficult to realize, and the full QPT with 4 and more qubits seems to be impractical.

The problem of exponential scaling of QPT resources with the number of qubits can be mitigated if we do not need full information about a quantum gate operation, but instead need only some information. Thus a partial characterization of a multi-qubit operation is an important area of theoretical research [22–28]. This includes randomized benchmarking [22, 29, 30], which typically provides only one number: the gate fidelity. Randomized benchmarking becomes increasingly preferable for superconducting qubits [31–33]. Another promising way to solve or at least alleviate the problem of exponential scaling is to use a compressed-sensing implementation of QPT [35–37].

One more problem with QPT is its sensitivity to state preparation and measurement errors (SPAM in the terminology of Ref. [31]). Randomized benchmarking does not suffer from SPAM-errors, so this is another reason why this technique is increasingly popular. However, the obvious drawback of randomized benchmarking is that it gives only the total (average) error and does not give any information about particular kinds of error. Hence, it does not tell us about the origin of a quantum gate imperfection.

In this paper we consider standard QPT, which gives full information about the quantum process. Because of the scaling problem, we are essentially talking about quantum gates with less than 4 qubits, for which full QPT is a very useful tool. The standard way of representing QPT results is via the process matrix χ [1] in the Pauli basis (see the next section). Unfortunately, this matrix is a rather inconvenient object to work with. Even though in principle it contains full information about the process, it does not show useful information in a straightforward way. Thus the important problem of converting experimental QPT data into a useful characterization of particular decoherence processes [8, 24, 26, 38–40] is not quite simple.

Besides the standard matrix χ , there are other ways to represent QPT results. For example, they can be represented via the so-called Pauli transfer matrix \mathcal{R} [34]. The advantage of using \mathcal{R} is that it contains only real elements, from \mathcal{R} it is simple to see whether the quantum operation is trace preserving, also simple to see whether the process is unital, and for any Clifford operation there is exactly one non-zero element in each row and column of \mathcal{R} with unit magnitude.

In this paper we discuss one more way of representing the experimental QPT results [41]. It is essentially the standard χ -matrix representation in the Pauli basis, with the only difference being that we factor out the desired unitary operation U , so that the error matrix χ^{err} de-

scribes only the imperfections of the experimental quantum gate. There are two natural ways to define such an error matrix (χ^{err} and $\tilde{\chi}^{\text{err}}$): we can assume that the U -operation is either before or after the error process (see Fig. 1 below). Even though in theoretical analyses it is rather usual to separate the error channel and unitary operation, we are not aware of any detailed discussion of the QPT representation by the error matrices. As discussed in this paper, the error matrix χ^{err} (as well as $\tilde{\chi}^{\text{err}}$) has a number of convenient properties. In particular, its main element is equal to the process fidelity F_χ , while other non-zero elements correspond to imperfections. Unitary imperfections are directly given by the imaginary parts of the elements along the left column and/or top row. Decoherence produces other elements, which have a relatively simple relation to Kraus operators characterizing decoherence (which are the operators in the Lindblad equation). Since the elements of the error matrix are small, most calculations can be approximated to first order, thus making them relatively simple. This includes a relatively simple rule for the composition of quantum operations and accumulation of the error-matrix elements due to the Lindblad-form decoherence. The error-matrix representation has already been used in the experimental QPT [21].

Our paper is organized in the following way. In Sec. II we briefly review some properties of the standard process matrix χ . In Sec. III we introduce the error matrices χ^{err} and $\tilde{\chi}^{\text{err}}$, and then in Sec. IV some of their properties are discussed, including physical interpretation. In Sec. V we consider composition of the error processes. Then in Sec. VI we discuss the use of the error matrix to find the necessary unitary correction to an experimental quantum gate. In Sec. VII we consider the contribution to the error matrix from decoherence described by the Lindblad-form master equation. A possible identification of SPAM errors and their subtraction from the error matrix are discussed in Sec. VIII. Finally, Sec. IX is the conclusion. Two appendices discuss topics that are somewhat different from the main text. In Appendix A we consider several simple examples of the χ -matrix calculation, and in Appendix B we discuss an intuitive interpretation of decoherence described by the Lindblad-form master equation, unraveling the quantum dynamics into the “jump” and “no jump” scenarios.

II. STANDARD PROCESS MATRIX χ

A linear quantum operation $\rho_{\text{in}} \rightarrow \rho_{\text{fin}}$ (transforming initial density matrix ρ_{in} into the final state ρ_{fin}) is usually described via the process matrix χ (which is Hermitian, with non-negative eigenvalues), defined as [1]

$$\rho_{\text{fin}} = \sum_{m,n} \chi_{mn} E_m \rho_{\text{in}} E_n^\dagger, \quad (1)$$

where the matrices E_n form a basis in the space of complex $d \times d$ matrices, which are the linear operators in the

d -dimensional Hilbert space of the problem. For example, for N qubits $d = 2^N$; therefore there are $(2^N)^2 = 4^N$ matrices E_n , and the matrix χ has dimensions $4^N \times 4^N$. (Note that E_n are operators in the space of wavefunctions, and these operators have the same dimension as density matrices.)

Even though in principle any basis $\{E_n\}$ (not necessarily orthogonal [42]) can be used in Eq. (1), the most usual choice for a system of qubits is the use of Pauli matrices. In this case for one qubit the basis $\{E_n\}$ consists of 4 matrices:

$$I \equiv \mathbb{1}, \quad X \equiv \sigma_x, \quad Y \equiv \sigma_y, \quad Z \equiv \sigma_z, \quad (2)$$

and for several qubits the Kronecker product of these matrices is used; for example for two qubits $\{E_n\} = \{II, IX, IY, IZ, XI, \dots, ZZ\}$. Note that sometimes a different definition for Y is used: $Y \equiv -i\sigma_y$. Also note that the basis of Pauli matrices is orthogonal (under the Hilbert-Schmidt inner product) but not normalized [42], so that

$$\langle E_m | E_n \rangle \equiv \text{Tr}(E_m^\dagger E_n) = \delta_{mn} d, \quad d = 2^N; \quad (3)$$

this is why normalization by d is often needed in the QPT. In this paper we will always assume the Pauli basis $\{E_n\}$ and use $Y \equiv \sigma_y$. Therefore $E_n^\dagger = E_n$, but for clarity we will still write E_n^\dagger in formulas when appropriate.

It is simple to find the matrix χ for a multi-qubit unitary operation U . We first need to find its representation in the Pauli basis, $U = \sum_n u_n E_n$, and then compare $U \rho_{\text{in}} U^\dagger$ with Eq. (1), which gives

$$\chi_{mn} = u_m u_n^*, \quad u_n = \frac{1}{d} \text{Tr}(U E_n^\dagger), \quad (4)$$

where the star notation means complex conjugation and the expression for u_n follows from the orthogonality property (3). Calculation of the matrix χ for a quantum process with decoherence is usually significantly more cumbersome. Some examples are considered in Appendix A (see also, e.g., [8]).

A process is called “trace-preserving” if the transformation (1) preserves the trace of the density matrix, i.e. if $\text{Tr}(\rho_{\text{fin}}) = 1$ when $\text{Tr}(\rho_{\text{in}}) = 1$. In this case the matrix χ should satisfy the condition $\sum_{m,n} \chi_{mn} E_n^\dagger E_m = \mathbb{1}$ (which gives 4^N real equations), and therefore χ is characterized by $16^N - 4^N$ real parameters instead of 16^N parameters in the general (non-trace-preserving) case. In this paper we always assume a trace-preserving operation.

The fidelity of a trace-preserving quantum operation compared with a desired unitary operation is usually defined as

$$F_\chi = \text{Tr}(\chi^{\text{des}} \chi), \quad (5)$$

where χ^{des} is for the desired unitary operation and χ is for the actual operation (it is easy to show that $0 \leq F_\chi \leq 1$). This definition has direct relation [43, 44]

$$1 - F_\chi = (1 - F_{\text{av}}) \frac{d+1}{d} \quad (6)$$

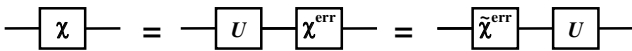


FIG. 1: Quantum circuit diagrams, which define the error processes characterized by error matrices χ^{err} and $\tilde{\chi}^{\text{err}}$ via their relation to χ and the desired unitary operation U . The time runs from left to right.

to the average state fidelity $F_{\text{av}} = \overline{\text{Tr}(\rho_{\text{fin}}\rho_{\text{fin}}^{\text{des}})}$, which assumes uniform averaging over all pure initial states. Sometimes [30] F_{av} is called “gate fidelity” while F_{χ} is called “process fidelity”. Characterization by F_{av} is usually used in randomized benchmarking [22, 29–32]; it is easy to see that $1/(d+1) \leq F_{\text{av}} \leq 1$.

Note that the fidelity definition (5) requires unitary desired operation and trace-preserving actual operation. For a general (non-unitary) desired operation (still assuming trace-preserving operations) it should be replaced with the “Uhlmann fidelity”

$$F_{\chi} = \left(\text{Tr} \sqrt{\sqrt{\chi} \chi^{\text{des}} \sqrt{\chi}} \right)^2 = \left(\text{Tr} \sqrt{\sqrt{\chi^{\text{des}}} \chi \sqrt{\chi^{\text{des}}}} \right)^2, \quad (7)$$

which is essentially the same definition as for the fidelity between two density matrices [1].

III. ERROR MATRICES χ^{err} AND $\tilde{\chi}^{\text{err}}$

The process matrix χ for a non-trivial unitary operation typically has many non-zero elements (e.g., 16 elements for the two-qubit controlled- Z , controlled-NOT, and $\sqrt{i\text{SWAP}}$ operations), and it is nice-looking on the standard bar (“cityscape”) chart used for visualization. However, a large number of non-zero elements (we will call them “peaks”) creates a problem in visual comparison between the desired and experimental χ -matrices, especially for high-fidelity experiments.

A natural way to make it easier to compare between the actual and desired operations is to show the difference between them, i.e., to show the error. For example, it is possible to calculate and display the difference $\chi - \chi^{\text{des}}$ in the Pauli basis. However, such element-by-element difference does not make much sense mathematically.

Instead, let us represent the actual quantum process as a *composition* of the desired unitary U and the error process (Fig. 1), and find the process matrix χ^{err} for this error operation. This essentially reduces the comparison between χ and desired U (we use a loose language here) to the comparison between χ^{err} and the memory (identity) operation.

So, the general idea is to convert the desired unitary U into the memory operation, and this converts χ into the error process matrix χ^{err} . There are two ways of defining such error matrix: we can place the error process either before or after the desired unitary U (Fig. 1). Thus, we define two error matrices: χ^{err} and $\tilde{\chi}^{\text{err}}$ using the

relations [see Eq. (1)]

$$\rho_{\text{fin}} = \sum_{m,n} \chi_{mn}^{\text{err}} E_m U \rho_{\text{in}} U^\dagger E_n^\dagger, \quad (8)$$

$$\rho_{\text{fin}} = \sum_{m,n} \tilde{\chi}_{mn}^{\text{err}} U E_m \rho_{\text{in}} E_n^\dagger U^\dagger. \quad (9)$$

From Fig. 1 it is obvious that the process χ^{err} can be represented as the composition of the inverse ideal unitary ($U^{-1} = U^\dagger$) and the actual process χ after that. Similarly, $\tilde{\chi}^{\text{err}}$ is the composition of χ and inverse unitary U^\dagger after that. Hence, χ^{err} and $\tilde{\chi}^{\text{err}}$ represent legitimate quantum processes and therefore they satisfy all the properties of the usual matrix χ (see the previous section); in particular, χ^{err} and $\tilde{\chi}^{\text{err}}$ are positive Hermitian matrices. We will use the standard Pauli basis for the error matrices χ^{err} and $\tilde{\chi}^{\text{err}}$.

Using the composition relation, the error matrices can be calculated from χ as [8]

$$\chi^{\text{err}} = V \chi V^\dagger, \quad V_{mn} = \text{Tr}(E_m^\dagger E_n U^\dagger)/d, \quad (10)$$

$$\tilde{\chi}^{\text{err}} = \tilde{V} \chi \tilde{V}^\dagger, \quad \tilde{V}_{mn} = \text{Tr}(E_m^\dagger U^\dagger E_n)/d. \quad (11)$$

In an experiment the error process matrices can be calculated either from χ using these equations or by directly applying the definitions (8) and (9) to the experimental data. For example, to find $\tilde{\chi}^{\text{err}}$ the measured final density matrices can be transformed numerically as $\rho_{\text{fin}} \rightarrow U^\dagger \rho_{\text{fin}} U$ and then the usual procedure of χ calculation can be applied. Note that the matrix χ^{err} can be thought of as the χ -matrix in the rotated basis $\{E_n U\}$ instead of $\{E_n\}$; similarly, $\tilde{\chi}^{\text{err}}$ is formally the χ -matrix in the basis $\{U E_n\}$; however, we will not use this language to avoid possible confusion.

In the ideal (desired) case both error processes χ^{err} and $\tilde{\chi}^{\text{err}}$ are equal to the perfect memory (identity) operation, $\chi^{\text{err}} = \tilde{\chi}^{\text{err}} = \chi^{\mathbf{I}}$, for which

$$\chi_{mn}^{\mathbf{I}} = \delta_{m0} \delta_{n0}, \quad (12)$$

where with index 0 we denote the left column and/or the top row, which correspond to the unity basis element (in the usual notation $0 = I$ for one qubit, $0 = II$ for two qubits, etc.); the process matrix (12) is given by Eq. (4) with $u_n = \delta_{n0}$. So, in the ideal case the error matrices have only one non-zero element at the top left corner: $\chi_{00}^{\text{err}} = \tilde{\chi}_{00}^{\text{err}} = 1$. Therefore, *any other non-zero element in χ^{err} (or $\tilde{\chi}^{\text{err}}$) indicates an imperfection of the quantum operation*. This is the main advantage in working with χ^{err} or $\tilde{\chi}^{\text{err}}$ instead of the usual matrix χ . There are also some other advantages discussed below.

The standard process fidelity (5) for a trace-preserving operation has a very simple form for the error matrices. Since χ , χ^{err} , and $\tilde{\chi}^{\text{err}}$ are essentially the same operator in different bases, we have $\text{Tr}(\chi^{\text{des}} \chi) = \text{Tr}(\chi^{\mathbf{I}} \chi^{\text{err}}) = \text{Tr}(\chi^{\mathbf{I}} \tilde{\chi}^{\text{err}})$. Therefore

$$F_{\chi} = \chi_{00}^{\text{err}} = \tilde{\chi}_{00}^{\text{err}}, \quad (13)$$

i.e. the process fidelity is just the height of the main (top left) element of the error matrix χ^{err} or $\tilde{\chi}^{\text{err}}$.

A systematic unitary error can be easily detected (to first order) in the error matrix χ^{err} or $\tilde{\chi}^{\text{err}}$ because it appears at a special location: it produces non-zero imaginary elements along the top row and left column of the matrix, i.e. the elements $\text{Im}(\chi_{0n}^{\text{err}}) = -\text{Im}(\chi_{n0}^{\text{err}})$ with $n \neq 0$ (similarly for $\tilde{\chi}^{\text{err}}$). To see this fact, let us assume that instead of the desired unitary operation U , the quantum gate actually realizes a slightly imperfect unitary U^{actual} . Then χ^{err} corresponds to the unitary $U^{\text{err}} = U^{\text{actual}}U^\dagger$, which can be expanded in the Pauli basis as $U^{\text{err}} = \sum_n u_n^{\text{err}} E_n$. Since $U^{\text{err}} \approx \mathbb{1}$, we have $u_0^{\text{err}} \approx 1$ and $|u_{n \neq 0}^{\text{err}}| \ll 1$. Note that u_0^{err} can always be chosen real because U^{err} is defined up to an overall phase. Now let us show that to first order all $u_{n \neq 0}^{\text{err}}$ are purely imaginary. This follows from the first-order expansion of the equation $U^{\text{err}}U^{\text{err}\dagger} = \mathbb{1}$, which gives $|u_0^{\text{err}}|^2 \mathbb{1} + \sum_{n \neq 0} (u_n^{\text{err}} + u_n^{\text{err}*}) E_n = \mathbb{1}$. Hence, $u_n^{\text{err}} + u_n^{\text{err}*} = 0$ for $n \neq 0$ (purely imaginary $u_{n \neq 0}^{\text{err}}$), and the difference $u_0^{\text{err}} - 1$ is only of second order (for a real u_0^{err}). Another way of showing that in the first order $u_{n \neq 0}^{\text{err}}$ are imaginary is by using representation $U^{\text{err}} = e^{iH_{\text{err}}}$ (neglecting the overall phase) with a Hermitian matrix H_{err} , so that the expansion $H_{\text{err}} = \sum_n h_n^{\text{err}} E_n$ contains all real coefficients, while to first order $u_{n \neq 0}^{\text{err}} = ih_{n \neq 0}^{\text{err}}$ and $u_0^{\text{err}} = 1$.

Now using Eq. (4) we see that to first order the only non-zero elements (except χ_{00}^{err}) are

$$\text{Im}(\chi_{n0}^{\text{err}}) = -\text{Im}(\chi_{0n}^{\text{err}}) \approx -iu_n^{\text{err}}, \quad n \neq 0. \quad (14)$$

Note that the diagonal elements χ_{nn}^{err} (as well as the change of χ_{00}^{err}) in this case are of second order. In particular, in this approximation $F_\chi \approx 1$. As discussed later, if decoherence causes a significant decrease of the fidelity F_χ , then a better approximation of the systematic unitary error effect is Eq. (14) multiplied by the fidelity,

$$\text{Im}(\chi_{n0}^{\text{err}}) \approx -iF_\chi u_n^{\text{err}}. \quad (15)$$

Using this equation it is possible to find u_n^{err} from an experimental matrix χ^{err} and therefore estimate the systematic unitary error U^{err} in the experiment.

The same property (14) [and its version (15) corrected for F_χ] can be shown for $\tilde{\chi}^{\text{err}}$ using the similar derivation for the unitary imperfection $\tilde{U}^{\text{err}} = U^\dagger U^{\text{actual}} \approx \mathbb{1}$. The elements $\text{Im}(\tilde{\chi}_{n0}^{\text{err}}) \approx -iF_\chi \tilde{u}_n^{\text{err}}$ are different compared with the matrix elements of χ^{err} ; they are related via the equation $\tilde{U}^{\text{err}} = U^\dagger U^{\text{err}} U$ or equivalent equation $\tilde{U}^{\text{err}} - \mathbb{1} = U^\dagger (U^{\text{err}} - \mathbb{1}) U$.

Decoherence produces additional small peaks in the error matrix χ^{err} (and/or $\tilde{\chi}^{\text{err}}$). As discussed later, to first order these peaks are linear in the decoherence strength and simply additive for different decoherence mechanisms. Therefore, to first order we have a weighted sum of different patterns in χ^{err} for different mechanisms. If these patterns for the most common decoherence mechanisms are relatively simple, then there is a rather straightforward way of extracting information on decoherence from experimental χ^{err} matrix. In Sec. VII

we will discuss the general way to calculate the first-order pattern for a particular decoherence mechanism; for a practical quantum gate this pattern may contain many elements. A special role is played by the real elements along the top row and left column of χ^{err} (or $\tilde{\chi}^{\text{err}}$): they correspond to the gradual non-unitary (“Bayesian”) evolution in the absence of the “jumps” due to decoherence (in contrast to the imaginary elements, which correspond to the unitary imperfection) – see discussion later.

Note that the diagonal matrix elements of χ^{err} are the error probabilities in the so-called Pauli twirling approximation [22, 45–47]. Therefore these elements can be used in simulation codes, which use the Pauli twirling approximation for the analysis of quantum algorithms in multi-qubit systems.

Concluding this section, we emphasize that the error matrix χ^{err} (and/or $\tilde{\chi}^{\text{err}}$) is just a minor modification of the standard χ matrix; they are related by a linear transformation and therefore equivalent to each other. However, in the error matrix only one peak (at the top left corner) corresponds to the desired operation, while other peaks indicate imperfections. This makes the error matrix more convenient to work with, when we analyze deviations of an experimental quantum operation from a desired unitary and try to extract information about the main decoherence mechanisms.

IV. SOME PROPERTIES OF THE ERROR MATRICES AND INTERPRETATION

In this paper we always assume high-fidelity operations,

$$1 - F_\chi \ll 1, \quad (16)$$

so that the first-order approximation of imperfections is quite accurate. Since the error matrix χ^{err} is positive, its off-diagonal elements have the upper bound

$$|\chi_{mn}^{\text{err}}| \leq \sqrt{\chi_{mm}^{\text{err}} \chi_{nn}^{\text{err}}}. \quad (17)$$

(The same is true for $\tilde{\chi}^{\text{err}}$, but for brevity we discuss here only χ^{err} .) Therefore for a high-fidelity operation (16) only the elements in the left column and top row can be relatively large, $|\chi_{0n}^{\text{err}}| = |\chi_{n0}^{\text{err}}| \leq \sqrt{\chi_{nn}^{\text{err}}} \leq \sqrt{1 - F_\chi}$, while other off-diagonal element have a smaller upper bound, $|\chi_{mn}^{\text{err}}| \leq (1 - F_\chi)/2$, because all diagonal elements except χ_{00}^{err} are small. Actually, it is possible to show (see below) that $\text{Re}(\chi_{0n}^{\text{err}})$ are also small, $|\text{Re}(\chi_{0n}^{\text{err}})| \leq (1 - F_\chi)/2$, so only $\text{Im}(\chi_{0n}^{\text{err}})$ can be relatively large.

The elements $\text{Im}(\chi_{0n}^{\text{err}})$ and $\text{Im}(\chi_{n0}^{\text{err}})$ play a special role because a unitary imperfection produce them in the first order, while other elements are of second order [see Eq. (4) and discussion in the previous section]. It is easy to see that $\text{Im}(\chi_{0n}^{\text{err}})$ and $\text{Im}(\chi_{n0}^{\text{err}})$ can approach $\pm\sqrt{\chi_{nn}^{\text{err}}}$ if the error is dominated by the unitary imperfection.

The physical intuition in analyzing the error of a quantum gate is that the (small) infidelity $1 - F_\chi$ comes from

small unitary imperfections and from rare but “strong” decoherence processes, which cause “jumps” that significantly change the state. As discussed later, this picture should also be complemented by small non-unitary state change in the case when no jump occurred (this change is essentially the quantum Bayesian update [48–50] due to the information that there was no jump).

It is not easy to formalize this intuition mathematically; however, there is a closely related procedure. Let us diagonalize the error matrix χ^{err} , so that

$$\chi^{\text{err}} = TDT^{-1}, \quad (18)$$

where T is a unitary $d^2 \times d^2$ matrix and $D = \text{diag}(\lambda_0, \lambda_1, \dots)$ is the diagonal matrix containing d^2 real eigenvalues of χ^{err} . These eigenvalues are non-negative, and we can always choose T so that in D they are ordered as $\lambda_0 \geq \lambda_1 \geq \dots \geq \lambda_{d^2-1}$. The sum of the eigenvalues is equal 1 (since we consider trace-preserving operations) and the largest eigenvalue λ_0 is close to 1 because $F_\chi \leq \lambda_0 \leq 1$. [Here $\lambda_0 \geq \chi_{00}^{\text{err}}$ because any diagonal element of a Hermitian matrix should be in between the largest and smallest eigenvalues, as follows from expanding the corresponding basis vector in the eigenbasis.] All other eigenvalues are small because $\sum_{k>0} \lambda_k \leq 1 - F_\chi$.

The diagonalization (18) directly gives the evolution representation via the Kraus operators [51],

$$\rho_{fin} = \sum_{k=0}^{d^2-1} \lambda_k A_k (U \rho_{in} U^\dagger) A_k^\dagger, \quad \sum_k \lambda_k A_k^\dagger A_k = \mathbb{1}, \quad (19)$$

$$A_k = \sum_n a_n^{(k)} E_n, \quad a_n^{(k)} = T_{nk}, \quad (20)$$

in which the operators A_k form an orthogonal basis, $\langle A_m | A_n \rangle = \delta_{mn} d$ [see Eq. (3)] because T is unitary. Recall that U is the desired unitary gate – see Eq. (8). The main term in the Kraus-operator representation (19) is the term with $\lambda_0 \approx 1$; let us show that $A_0 \approx \mathbb{1}$ (up to an overall phase, which can always be eliminated); this means $a_0^{(0)} \approx 1$ and $|a_n^{(0)}| \ll 1$ for $n \neq 0$ [note that $\sum_n |a_n^{(0)}|^2 = 1$ because T is unitary; therefore it is sufficient to show that $a_0^{(0)} \approx 1$]. This can be done in the following way. Since

$$\chi_{mn}^{\text{err}} = \sum_k \lambda_k a_m^{(k)} (a_n^{(k)})^*, \quad (21)$$

the fidelity is

$$F_\chi = \sum_k \lambda_k |a_0^{(k)}|^2. \quad (22)$$

The contribution of the terms with $k \neq 0$ to the fidelity is at least smaller than $1 - F_\chi$ because this is the bound for $\sum_{k>0} \lambda_k$ and $|a_0^{(k)}| = |T_{0k}| < 1$ for a unitary T (this contribution is actually even much smaller, as discussed below). Therefore $\lambda_0 |a_0^{(0)}|^2 > 2F_\chi - 1$, and so $|a_0^{(0)}|^2 > 1 - 2(1 - F_\chi)$. Choosing real $a_0^{(0)}$, we obtain $a_0^{(0)} \approx 1$, and therefore $A_0 \approx E_0 = \mathbb{1}$.

Since A_0 is close to E_0 and other A_k are orthogonal to A_0 , the components $a_0^{(k)}$ are small for $k \neq 0$. Using the relation $(a_0^{(0)})^* a_0^{(k)} + \sum_{n>0} (a_n^{(0)})^* a_n^{(k)} = 0$ (since T is unitary), we find the bound $|a_0^{(k)}| < \sqrt{\sum_{n>0} |a_n^{(0)}|^2} \sqrt{\sum_{n>0} |a_n^{(k)}|^2} / |a_0^{(0)}|$. Now using $|a_0^{(0)}| \approx 1$, $\sum_{n>0} |a_n^{(k)}|^2 \leq 1$, and $\sum_{n>0} |a_n^{(0)}|^2 < 2(1 - F_\chi)$ (see the previous paragraph), we obtain $|a_0^{(k)}|^2 < 2(1 - F_\chi)$, neglecting the terms of the order $(1 - F_\chi)^3$. This means that the contribution to the fidelity (22) from the Kraus operators with $k > 0$ is limited at least by $2(1 - F_\chi)^2$ [neglecting the order $(1 - F_\chi)^4$], and therefore a good approximation for the fidelity is

$$F_\chi \approx \lambda_0 |a_0^{(0)}|^2, \quad 1 - F_\chi \approx (1 - |a_0^{(0)}|^2) + (1 - \lambda_0), \quad (23)$$

which corresponds to the intuitive separation of the infidelity $1 - F_\chi$ into the “coherent” error $1 - |a_0^{(0)}|^2$ and the error $1 - \lambda_0$ due to rare but strong decoherence “jumps”.

Thus the Kraus-operator representation (19) can be crudely interpreted in the following way. After the desired unitary U , we apply the Kraus operator $A_0 \approx \mathbb{1}$ with the probability $\lambda_0 \approx 1$, while with small remaining probabilities λ_k we apply very different (orthogonal to A_0) Kraus operators A_k . Imperfection of A_0 (compared with $\mathbb{1}$) leads to the “coherent” error $1 - |a_0^{(0)}|^2$ with $a_0^{(0)} = \text{Tr}(A_0)/d$. Other Kraus operators are practically orthogonal to $E_0 = \mathbb{1}$, so they correspond to “strong decoherence” and practically always lead to an error, which happens with the total probability $\sum_k \lambda_k = 1 - \lambda_0$, thus explaining Eq. (23). While this interpretation seems to be quite intuitive, there are two caveats. First, it is incorrect to say that A_k is applied with the probability λ_k . Instead, we should say [1, 51] that the evolution scenario

$$|\psi_{in}\rangle \rightarrow \frac{A_k U |\psi_{in}\rangle}{\text{Norm}}, \quad \rho_{in} \rightarrow \frac{A_k U \rho_{in} U^\dagger A_k^\dagger}{\text{Norm}} \quad (24)$$

occurs with the probability $P_k = \lambda_k \text{Tr}(A_k^\dagger A_k U \rho_{in} U^\dagger)$, which depends on the initial state and is equal to λ_k only on average, $\overline{P_k} = \lambda_k$, after averaging over pure initial states. [This can be proven by using $\overline{\rho_{in}} = \mathbb{1}/d$ and $\text{Tr}(A_k^\dagger A_k) = d$.] Note that the operators A_k can violate the inequality $A_k^\dagger A_k \leq \mathbb{1}$, even though $\lambda_k A_k^\dagger A_k \leq \mathbb{1}$ is always satisfied. The second caveat is that A_0 is not necessarily unitary, as would be naively expected for the separation into a coherent operation and decoherence. The non-unitary part of A_0 can be interpreted as due to the absence of jumps $A_{k>0}$, similar to the null-result evolution [48, 50] (see below and also discussions in Sec. VII and Appendix B). We may include both contributions (imperfect unitary part and non-unitary part of A_0) into what we call the “coherent error”, so it is characterized by the difference between A_0 and $\mathbb{1}$ (probably it is better to call it the “gradual error”). With understanding of these two caveats, the discussed above interpretation of the Kraus representation (19) can be useful for gaining some intuition.

Note that the contribution to χ^{err} [see Eq. (21)] from the imperfection of the main Kraus operator A_0 mainly causes the elements $\chi_{n0}^{\text{err}} = (\chi_{0n}^{\text{err}})^* \approx \lambda_0 a_n^{(0)}$ in the top row and left column of the error matrix (other elements are of the second order in the imperfection). In contrast, other (“decoherence jump”) operators A_k mainly produce other elements of χ^{err} ; their contribution to χ_{0n}^{err} is limited by $\sqrt{2}(1 - F_\chi)\sqrt{\chi_{nn}^{\text{err}}}$, as follows from the positivity of $\chi_{mn}^{\text{dec}} \equiv \sum_{k>0} \lambda_k a_m^{(k)} (a_n^{(k)})^*$, which gives $|\chi_{0n}^{\text{dec}}| \leq \sqrt{\chi_{00}^{\text{dec}} \chi_{nn}^{\text{dec}}}$, and the derived above inequality $\chi_{00}^{\text{dec}} \leq 2(1 - F_\chi)^2$. Significant contributions to the diagonal elements of χ^{err} may come from both A_0 and $A_{k>0}$.

Therefore, we can apply the following approximate procedure to crudely separate the error matrix,

$$\chi^{\text{err}} = \chi^{\text{coh}} + \chi^{\text{dec}}, \quad \chi_{mn}^{\text{coh}} = \lambda_0 a_m^{(0)} (a_n^{(0)})^*, \quad (25)$$

into the “coherent” (or “gradual”) part $\lambda_0 a_m^{(0)} (a_n^{(0)})^*$ and “strong decoherence” χ^{dec} [see Eq. (21)]. We first estimate the “coherent probability” λ_0 as

$$\lambda_0 \approx F_\chi / \left(1 - \sum_{n>0} |\chi_{0n}^{\text{err}}|^2\right), \quad (26)$$

and then use this λ_0 in the estimation $a_{n>0}^{(0)} \approx \chi_{n0}^{\text{err}} / \lambda_0$. Using λ_0 and $a_n^{(0)}$ we can construct χ^{coh} , while the remaining part of χ^{err} is χ^{dec} . The diagonal elements χ_{nn}^{err} with $n \neq 0$ (error probabilities) are thus separated into the contributions $\lambda_0 |a_n^{(0)}|^2$ from the “coherent imperfection” and $\chi_{nn}^{\text{err}} - \lambda_0 |a_n^{(0)}|^2$ due to “strong decoherence”. A further simplification of this procedure is to approximate the coherent part as $\chi_{mn}^{\text{coh}} \approx \chi_{m0}^{\text{err}} (\chi_{0n}^{\text{err}})^*$ for $m \neq 0, n \neq 0$, and $\chi_{m0}^{\text{coh}} = (\chi_{0m}^{\text{coh}})^* \approx \chi_{m0}^{\text{err}}$.

One more useful approach for the intuitive understanding of χ^{err} elements along the left column and top row is the following. Using the completeness relation (19) we can write the main (“coherent”) Kraus operator in the polar decomposition representation as

$$\sqrt{\lambda_0} A_0 = U^{\text{err}} \sqrt{\mathbb{1} - \sum_{k>0} \lambda_k A_k^\dagger A_k} \quad (27)$$

$$\approx U^{\text{err}} \left(\mathbb{1} - \frac{1}{2} \sum_{k>0} \lambda_k A_k^\dagger A_k \right), \quad (28)$$

where $U^{\text{err}} \approx \mathbb{1}$ is some unitary, which corresponds to the unitary imperfection [since the overall phase is arbitrary, we can choose $\text{Im}(\text{Tr}(U^{\text{err}})) = 0$]. Then let us expand the operators in the Pauli basis,

$$U^{\text{err}} \approx (1 - \frac{1}{2} \mathcal{E}_U) E_0 + \sum_{n>0} u_n^{\text{err}} E_n, \quad \mathcal{E}_U \equiv \sum_{n>0} |u_n^{\text{err}}|^2, \quad (29)$$

$$\sum_{k>0} \lambda_k A_k^\dagger A_k = \mathcal{E}_D E_0 + \sum_{n>0} g_n E_n, \quad \mathcal{E}_D \equiv 1 - \lambda_0, \quad (30)$$

where u_n^{err} and g_n are the expansion components, and we introduced the naturally defined unitary error \mathcal{E}_U and decoherence error \mathcal{E}_D (average probability of “jumps”).

Now using Eq. (23) and neglecting the second-order products $u_m^{\text{err}} g_n$, we find the intuitively expected formula for fidelity,

$$F_\chi \approx 1 - \mathcal{E}_U - \mathcal{E}_D. \quad (31)$$

Similarly, taking into account only the contribution from the main Kraus operator, for the elements $\chi_{n0}^{\text{err}} = \chi_{0n}^{\text{err}*}$ with $n \neq 0$ we find

$$\chi_{n0}^{\text{err}} \approx (1 - \frac{1}{2} \mathcal{E}_U - \mathcal{E}_D) u_n^{\text{err}} + (1 - \mathcal{E}_U - \frac{1}{2} \mathcal{E}_D) \frac{g_n}{2}. \quad (32)$$

Here u_n^{err} are purely imaginary (in the first order) because U^{err} is unitary, while g_n are real because Eq. (30) is the expansion of a Hermitian operator. Therefore, we see that the imaginary parts of the elements χ_{n0}^{err} are due to unitary imperfection, while their real parts come from the absence of “jumps” (described by Kraus operators with $k > 0$) via Eq. (27). It is easy to see that the evolution $\sqrt{\mathbb{1} - \sum_{k>0} \lambda_k A_k^\dagger A_k}$ is essentially the Bayesian update of the quantum state [48–50] due the absence of jumps.

In experiments with superconducting qubits the quantum gate infidelity is usually dominated by decoherence, $\mathcal{E}_D \gg \mathcal{E}_U$, unless the unitary part is very inaccurate. We will often assume this situation implicitly. In this case case $F_\chi \approx 1 - \mathcal{E}_D$, and from Eq. (32) we obtain Eq. (15).

Using Eqs. (30) and (32) we can show the bound $|\text{Re}(\chi_{n0}^{\text{err}})| \leq (1 - \lambda_0)/2 \leq (1 - F_\chi)/2$. The starting point is to see that all components of $A_k^\dagger A_k$ in the Pauli basis are not larger than 1, i.e. $|\text{Tr}(E_n^\dagger A_k^\dagger A_k)/d| \leq 1$ for any n . This is because $A_k^\dagger A_k = \sum_{m,l} (a_m^{(k)})^* E_m^\dagger a_l^{(k)} E_l$ and the product of two Pauli operators is a Pauli operator (with a phase factor); therefore a particular (say, n th) component is essentially a sum of pairwise products of the “vector coordinates” $(a_m^{(k)})^*$ and the same coordinates $a_l^{(k)}$ in a different order (also, with phase factors). Therefore, the sum of products is limited by the norms of the two vectors, which is 1 for both vectors ($\sum_m |a_m^{(k)}|^2 = 1$). Since the Pauli-basis components of $A_k^\dagger A_k$ are limited by 1, the sum of k th contributions to g_n in Eq. (30) is limited by $|g_n| \leq \sum_{k>0} \lambda_k = 1 - \lambda_0$. This gives $|\text{Re}(\chi_{n0}^{\text{err}})| \leq (1 - \lambda_0)/2$ via Eq. (32).

Since the elements $\text{Re}(\chi_{n0}^{\text{err}})$ are small, so that their second-order contributions to the diagonal elements are practically negligible, $[\text{Re}(\chi_{n0}^{\text{err}})]^2 \leq (1 - F_\chi)^2/4$, it does not matter much whether we include the evolution due to the “no-jump” Bayesian update into the “coherent part” (25) or not. Note that this Bayesian evolution does not produce an additional error since $\text{Tr}[E_0^\dagger (1 - \frac{1}{2} \sum_{k>0} \lambda_k A_k^\dagger A_k)]/d = 1 - \frac{1}{2} \sum_{k>0} \lambda_k = 1 - (1 - \lambda_0)/2$ and therefore from Eq. (27) we see that $a_0^{(0)} \approx 1 - \frac{1}{2} \sum_{k>0} |u_k^{\text{err}}|^2$, i.e. the “no-jump” scenario brings only the unitary error.

In this section we discussed only the error matrix χ^{err} ; however, the same analysis can be also applied to $\tilde{\chi}^{\text{err}}$.

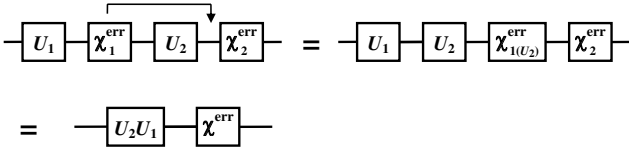


FIG. 2: Quantum circuit diagram for the composition of two quantum operations. The arrow illustrates “jumping” the error process χ_1^{err} over the unitary U_2 .

The relation between the error matrices is [8]

$$\chi^{\text{err}} = W_{(U)} \tilde{\chi}^{\text{err}} W_{(U)}^\dagger, \quad \tilde{\chi}^{\text{err}} = W_{(U)}^\dagger \chi^{\text{err}} W_{(U)}, \quad (33)$$

where the unitary matrix $W_{(U)}$ corresponds to the effective change of the basis $\{E_n\}$ due to U ,

$$W_{(U),mn} = \text{Tr}(E_m^\dagger U E_n U^\dagger)/d. \quad (34)$$

Note that $W_{(U)}^\dagger = W_{(U^\dagger)}$. It is convenient to think that the W -transformation (33) is due to the error matrix “jumping over” the unitary U (see Fig. 1). It is easy to see from Eq. (34) that $W_{0n} = \delta_{0n}$; therefore for an ideal memory $W\chi^{\text{I}}W^\dagger = \chi^{\text{I}}$ and Eq. (33) essentially transforms only the difference from the ideal memory.

The W^\dagger -transformation $\chi^{\text{err}} \rightarrow \tilde{\chi}^{\text{err}}$ (33) obviously corresponds to the unitary transformation of Kraus operators A_k , “jumping over” U to the left (Fig. 1),

$$\tilde{A}_k = U^\dagger A_k U. \quad (35)$$

These \tilde{A}_k form the Kraus-operator representation of $\tilde{\chi}^{\text{err}}$ with the same “probabilities” λ_k .

V. COMPOSITION OF ERROR PROCESSES

Let us calculate the error matrix χ^{err} for the composition of two quantum operations: desired unitary U_1 with error process χ_1^{err} and after that the desired unitary U_2 with error χ_2^{err} (Fig. 2). It is obvious that the resulting desired unitary is $U_2 U_1$ (note that the matrix multiplication is from right to left, while on the quantum circuit diagrams the time runs from left to right). We assume sufficiently high fidelity of both operations, $F_1 \simeq 1$, $F_2 \simeq 1$ [for brevity we omit the subscript χ in the notation (13) for fidelity].

Let us start with the simple case when there are no unitaries, $U_1 = U_2 = \mathbb{1}$. Then the relation between the initial state ρ_{in} and the final state ρ_{fin} is

$$\rho_{\text{fin}} = \sum_{m,n,p,q} \chi_{1,mn}^{\text{err}} \chi_{2,pq}^{\text{err}} E_p E_m \rho_{\text{in}} E_n^\dagger E_q^\dagger, \quad (36)$$

which leads to the usual lengthy expression for the composition of two operations:

$$\chi_{ab}^{\text{err}} = \sum_{m,n,p,q} \chi_{1,mn}^{\text{err}} \chi_{2,pq}^{\text{err}} \frac{1}{d^2} \text{Tr}(E_p E_m E_a^\dagger) \text{Tr}(E_q E_n E_b^\dagger)^*, \quad (37)$$

where we used relation

$$E_p E_m = \sum_a \frac{1}{d} \text{Tr}(E_p E_m E_a^\dagger) E_a \quad (38)$$

(actually there is only one non-zero term in this relation, but there is no simple way to write it). Equation (37) is valid for any two operations (not necessarily error processes) and is very inconvenient to use. Fortunately, it is greatly simplified for the error processes, since χ_1^{err} and χ_2^{err} contain only one large (close to one) element, $\chi_{1,00}^{\text{err}} = F_1$ and $\chi_{2,00}^{\text{err}} = F_2$, while all other elements are small. Therefore we can use the first order approximation of Eq. (37), which gives the simple additive relation

$$\chi_{mn}^{\text{err}} \approx F_2 \chi_{1,mn}^{\text{err}} + F_1 \chi_{2,mn}^{\text{err}} \quad (39)$$

$$\approx \chi_{1,mn}^{\text{err}} + \chi_{2,mn}^{\text{err}} \quad (40)$$

for all elements except the main element χ_{00}^{err} . The approximation (40) can also be written as

$$\chi^{\text{err}} \approx \chi_1^{\text{err}} + \chi_2^{\text{err}} - \chi^{\text{I}}. \quad (41)$$

Obviously, it is much easier to deal with the composition of error processes than with the composition of general quantum processes. Note that Eq. (39) can also be naturally understood using the Kraus-operator representation (19) in the case when infidelity is dominated by decoherence.

The approximation (39) neglects the second-order corrections due to possibly significant coherent errors. While this is good enough for the off-diagonal elements of χ^{err} , let us use a better approximation for the more important diagonal elements (except χ_{00}^{err}), explicitly taking into account the top rows and left columns of χ_1^{err} and χ_2^{err} in Eq. (37),

$$\chi_{nn}^{\text{err}} \approx F_2 \chi_{1,nn}^{\text{err}} + F_1 \chi_{2,nn}^{\text{err}} + 2 \text{Im}(\chi_{1,0n}^{\text{err}}) \text{Im}(\chi_{2,0n}^{\text{err}}), \quad (42)$$

where the formally similar term $2 \text{Re}(\chi_{1,0n}^{\text{err}}) \text{Re}(\chi_{2,0n}^{\text{err}})$ is neglected, because the elements $\text{Re}(\chi_{0n}^{\text{err}})$ cannot be relatively large, in contrast to $\text{Im}(\chi_{0n}^{\text{err}})$.

For the fidelity the exact and approximate results are

$$F_\chi = \chi_{00}^{\text{err}} = \sum_{m,n} \chi_{1,mn}^{\text{err}} \chi_{2,mn}^{\text{err}} \quad (43)$$

$$\approx F_1 F_2 - 2 \sum_{n \neq 0} \text{Im}(\chi_{1,0n}^{\text{err}}) \text{Im}(\chi_{2,0n}^{\text{err}}), \quad (44)$$

where the similar term $-2 \sum_{n \neq 0} \text{Re}(\chi_{1,0n}^{\text{err}}) \text{Re}(\chi_{2,0n}^{\text{err}})$ is neglected again. Note that $\text{Tr}(\chi^{\text{err}})$ calculated using approximations (42) and (44) is slightly smaller than 1, but the difference is of second order in infidelity.

The reason for taking a special care of the elements $\text{Im}(\chi_{1,0n}^{\text{err}})$ and $\text{Im}(\chi_{2,0n}^{\text{err}})$ becomes clear if we consider the composition of small unitaries U_1^{err} and U_2^{err} . Then the approximate addition (40) is valid for the first-order off-diagonal elements of χ^{err} (which are in the left column and top row); however, the diagonal elements are of second order, and for them the errors

add up “coherently”, generating the “interference” term $2\text{Im}(\chi_{1,0n}^{\text{err}})\text{Im}(\chi_{2,0n}^{\text{err}})$ in Eq. (42). Note that the neglected terms $2\text{Re}(\chi_{1,0n}^{\text{err}})\text{Re}(\chi_{2,0n}^{\text{err}})$ have a somewhat similar origin, considering the “coherent” composition of the main (“no-jump”) Kraus operators in the representation (19).

We emphasize that Eqs. (39)–(44) do not change if we exchange the sequence of χ_1^{err} and χ_2^{err} . So in this approximation small imperfections of quantum “memory” operations commute with each other, as intuitively expected. Note that for the fidelity (43) this result is exact: commutation of arbitrary error processes does not change F_χ .

So far we assumed $U_1 = U_2 = \mathbb{1}$. Now let us consider arbitrary desired unitaries U_1 and U_2 . Then χ^{err} for the composition can be calculated in two steps (see Fig. 2): we first exchange the sequence of χ_1^{err} and U_2 , thus producing the effective error process $\chi_{1(U_2)}^{\text{err}}$, and then use the discussed above rule for the composition of two “memory” operations $\chi_{1(U_2)}^{\text{err}}$ and χ_2^{err} . The transformation of χ_1^{err} when it “jumps over” U_2 (Fig. 2) is essentially the same as the transformation between $\tilde{\chi}^{\text{err}}$ and χ^{err} [see Fig. 1] and is given by the equation

$$\chi_{1(U_2)}^{\text{err}} = W_{(U_2)}\chi_1^{\text{err}}W_{(U_2)}^\dagger, \quad (45)$$

where $W_{(U_2)}$ is given by Eq. (34). This transformation can also be written as

$$\chi_{1(U_2)}^{\text{err}} = \chi^{\mathbf{I}} + W_{(U_2)}(\chi_1^{\text{err}} - \chi^{\mathbf{I}})W_{(U_2)}^\dagger, \quad (46)$$

so that only the small difference from the ideal memory operation $\chi^{\mathbf{I}}$ is being transformed. Note that this transformation does not change fidelity, $\chi_{1(U_2),00}^{\text{err}} = \chi_{1,00}^{\text{err}} = F_1$.

Thus we have a relatively simple procedure to find χ^{err} for the composition of two quantum operations: we first apply the transformation (45) to move the two error processes together (Fig. 2) and then apply approximate rules (39)–(44) to the matrices $\chi_{1(U_2)}^{\text{err}}$ and χ_2^{err} .

The similar procedure can be used to calculate $\tilde{\chi}^{\text{err}}$ for the composition of two quantum operations. We should first move $\tilde{\chi}_2^{\text{err}}$ to the left by jumping it over U_1 ,

$$\tilde{\chi}_{2(U_1)}^{\text{err}} = W_{(U_1)}^\dagger\tilde{\chi}_2^{\text{err}}W_{(U_1)}, \quad (47)$$

and then use the approximate composition rules (39)–(44) for the error matrices χ_1^{err} and $\tilde{\chi}_{2(U_1)}^{\text{err}}$.

For the composition of several quantum operations χ_i^{err} , the error processes should be first moved to the end of the sequence by jumping them over the desired unitaries (or moved to the beginning if we consider the language of $\tilde{\chi}^{\text{err}}$) and then we use the composition rules (39)–(44). The procedure further simplifies if we can neglect “coherent” errors and use the simple additive rule (40) for all elements (except $\chi_{00}^{\text{err}} = 1 - \sum_{n \neq 0} \chi_{nn}^{\text{err}}$).

VI. UNITARY CORRECTIONS

In experiments it is often useful to check how large the inaccuracy is of the unitary part of a realized quantum gate and find the necessary unitary corrections to improve fidelity of the gate. The error matrix χ^{err} (or $\tilde{\chi}^{\text{err}}$) gives us a simple way to do this, because small unitary imperfections directly show up as the imaginary parts of the elements χ_{0n}^{err} and χ_{n0}^{err} .

Let us assume that we apply a small unitary correction $U^{\text{corr}} = \sum_n u_n^{\text{corr}}E_n \approx \mathbb{1}$ after an operation characterized by the desired U and error matrix χ^{err} with fidelity F_χ . Then the process matrix $\chi_{mn}^{\text{corr}} = u_m^{\text{corr}}u_n^{\text{corr}*}$ for the correction operation mainly consists of the element $\chi_{00}^{\text{corr}} \approx 1$ and the imaginary first-order elements $\chi_{n0}^{\text{corr}} \approx \chi_{0n}^{\text{corr}*} \approx u_n^{\text{corr}}$ [see Eq. (14)], while all other elements are of second order. Using Eq. (42) we see that after the correction the elements in the left column of the error matrix approximately change as

$$\chi_{n0}^{\text{err}} \rightarrow \chi_{n0}^{\text{err}} + F_\chi u_n^{\text{corr}}, \quad (48)$$

so to correct the unitary imperfection we need to choose

$$u_n^{\text{corr}} \approx -i\text{Im}(\chi_{n0}^{\text{err}})/F_\chi, \quad (49)$$

which cancels the imaginary part of the left-column elements (here the factor F_χ^{-1} needs an implicit assumption that the infidelity is dominated by decoherence). The increase of the gate fidelity ΔF_χ due to this correction procedure can be estimated using Eq. (44),

$$\Delta F_\chi \approx \sum_{n \neq 0} (\text{Im} \chi_{n0}^{\text{err}})^2 / F_\chi. \quad (50)$$

In this derivation the factor of 2 in the second term of Eq. (44) is compensated by the fidelity decrease due to the first term. The result (50) in the case $F_\chi \approx 1$ coincides with what we would expect from the unitary correction in absence of decoherence. The factor F_χ^{-1} in Eq. (50) implicitly assumes that the infidelity is dominated by decoherence.

Note that the fidelity increase ΔF_χ is of second order, so in an experiment we should not expect a significant improvement of fidelity due to unitary correction, unless the unitary imperfection is quite big. Also note that in an experiment it may be easy to apply a unitary correction only in some “directions”, for example, by applying single-qubit pulses, while other corrections may be very difficult. In this case only some of the elements $\text{Im}(\chi_{n0}^{\text{err}})$ can be compensated, and then the fidelity improvement is given by Eq. (50), in which summation is only over the elements, compensated by the correction procedure.

The above analysis of the compensation procedure assumes a small compensation. If the unitary error is large, then to find the optimal correction U^{corr} we can use an iterative procedure, in which we first estimate the correction via Eq. (49), then use the exact composition relation (37), and then again adjust the correction via Eq. (49).

Our analysis of the unitary compensation procedure assumed application of U^{corr} after the quantum gate. If the compensation is applied before the quantum gate, then it is more natural to use the language of $\tilde{\chi}^{\text{err}}$ (see Fig. 1); in this case Eqs. (48)–(50) remain valid, with χ^{err} replaced by $\tilde{\chi}^{\text{err}}$. Applying corrections both before and after the gate may in some cases increase the number of correctable “directions” in the space of unitary operators.

To illustrate analysis of the unitary corrections, let us consider the two-qubit controlled-Z (CZ) gate in the “quantum von Neumann architecture” [52–54], in which single-qubit Z -rotations are realizable very easily (without an additional cost), and so such corrections can be easily applied. Application of Z -rotation over the small angle φ_1 to the first qubit and Z -rotation over the small angle φ_2 to the second qubit produces the correction unitary $U^{\text{corr}} = \text{diag}(1, e^{i\varphi_1}, e^{i\varphi_2}, e^{i\varphi_3})$ in the basis $\{|00\rangle, |10\rangle, |01\rangle, |11\rangle\}$. Here $\varphi_3 = \varphi_1 + \varphi_2$, but if we can also introduce correction φ_{CZ} of the CZ angle, then it will be $\varphi_3 = \varphi_1 + \varphi_2 + \varphi_{CZ}$. Expansion of U^{corr} in the Pauli basis gives four non-zero elements:

$$u_{II}^{\text{corr}} = \frac{1}{d} \text{Tr}(U^{\text{corr}} \times II) = \frac{1}{4}(1 + e^{i\varphi_1} + e^{i\varphi_2} + e^{i\varphi_3}) \approx 1 + i(\varphi_1 + \varphi_2 + \varphi_3)/4, \quad (51)$$

$$u_{IZ}^{\text{corr}} = \frac{1}{d} \text{Tr}(U^{\text{corr}} \times IZ) = \frac{1}{4}(1 - e^{i\varphi_1} + e^{i\varphi_2} - e^{i\varphi_3}) \approx i(-\varphi_1 + \varphi_2 - \varphi_3)/4, \quad (52)$$

$$u_{ZI}^{\text{corr}} = \frac{1}{d} \text{Tr}(U^{\text{corr}} \times ZI) \approx \frac{i}{4}(\varphi_1 - \varphi_2 - \varphi_3), \quad (53)$$

$$u_{ZZ}^{\text{corr}} = \frac{1}{d} \text{Tr}(U^{\text{corr}} \times ZZ) \approx \frac{i}{4}(-\varphi_1 - \varphi_2 + \varphi_3), \quad (54)$$

where we used the standard notation for the two-qubit operator basis $\{II, IX, IY, IZ, XI, \dots, ZZ\}$; note that the index 0 in the notations of our paper corresponds to II .

It is important to emphasize that this expansion of U^{corr} is not exactly what we used in Eqs. (48) and (49) because we assumed real $u_0^{\text{corr}} \approx 1$, while u_{II}^{corr} in Eq. (51) is not real. We therefore need to adjust the overall phase of U^{corr} to make u_{II}^{corr} real. This can be easily done by replacing U^{corr} with $U^{\text{corr}} e^{-i(\varphi_1 + \varphi_2 + \varphi_3)/4}$. However, for small angles φ_i this would produce only a small change in Eqs. (52)–(54). The left column of χ^{corr} therefore contains the same non-zero elements,

$$\chi_{IZ,II}^{\text{corr}} \approx i(-\varphi_1 + \varphi_2 - \varphi_3)/4 = i(-2\varphi_1 - \varphi_{CZ})/4, \quad (55)$$

$$\chi_{ZI,II}^{\text{corr}} \approx i(\varphi_1 - \varphi_2 - \varphi_3)/4 = i(-2\varphi_2 - \varphi_{CZ})/4, \quad (56)$$

$$\chi_{ZZ,II}^{\text{corr}} \approx i(-\varphi_1 - \varphi_2 + \varphi_3)/4 = i\varphi_{CZ}/4. \quad (57)$$

If we correct only φ_1 and φ_2 (so that $\varphi_{CZ} = 0$), then we should choose them [see Eq. (49)] as

$$\varphi_1 \approx 2 \text{Im}(\chi_{IZ,II}^{\text{err}})/F_\chi, \quad \varphi_2 \approx 2 \text{Im}(\chi_{ZI,II}^{\text{err}})/F_\chi, \quad (58)$$

where χ^{err} and $F_\chi = \chi_{II,II}^{\text{err}}$ are measured experimentally. This will cancel the left-column elements

$\text{Im}(\chi_{IZ,II}^{\text{err}})$ and $\text{Im}(\chi_{ZI,II}^{\text{err}})$ in the corrected quantum gate and produce fidelity improvement $\Delta F_\chi \approx [(\text{Im}\chi_{IZ,II}^{\text{err}})^2 + (\text{Im}\chi_{ZI,II}^{\text{err}})^2]/F_\chi$.

If we can also correct φ_{CZ} , then we should choose corrections

$$\varphi_1 \approx 2 \text{Im}(\chi_{IZ,II}^{\text{err}} + \chi_{ZZ,II}^{\text{err}})/F_\chi, \quad (59)$$

$$\varphi_2 \approx 2 \text{Im}(\chi_{ZI,II}^{\text{err}} + \chi_{ZZ,II}^{\text{err}})/F_\chi, \quad (60)$$

$$\varphi_{CZ} \approx -4 \text{Im}(\chi_{ZZ,II}^{\text{err}})/F_\chi. \quad (61)$$

This will cancel the left-column elements $\text{Im}(\chi_{IZ,II}^{\text{err}})$, $\text{Im}(\chi_{ZI,II}^{\text{err}})$, and $\text{Im}(\chi_{ZZ,II}^{\text{err}})$ in the corrected quantum gate and produce fidelity improvement $\Delta F_\chi \approx [(\text{Im}\chi_{IZ,II}^{\text{err}})^2 + (\text{Im}\chi_{ZI,II}^{\text{err}})^2 + (\text{Im}\chi_{ZZ,II}^{\text{err}})^2]/F_\chi$.

Note that U^{corr} commutes with the CZ gate, $U^{CZ} = \text{diag}(1, 1, 1, -1)$, so it does not matter if the single-qubit corrections are applied before or after the gate (the φ_{CZ} correction is obviously a correction of the gate itself). Similarly, it does not matter if we use χ^{err} or $\tilde{\chi}^{\text{err}}$ in this correction procedure.

VII. ERROR MATRIX FROM THE LINDBLAD-FORM DECOHERENCE

Let us consider a quantum evolution described by the Lindblad-form master equation

$$\dot{\rho} = -\frac{i}{\hbar}[H, \rho] + \sum_j \Gamma_j (B_j \rho B_j^\dagger - \frac{1}{2} B_j^\dagger B_j \rho - \frac{1}{2} \rho B_j^\dagger B_j), \quad (62)$$

where $H(t)$ is the Hamiltonian (which has a significant time dependence for a multi-stage quantum gate) and j th decoherence mechanism is described by the Kraus operator B_j and the rate $\Gamma_j(t)$. Mathematically it is natural to work with the combination $\sqrt{\Gamma_j} B_j$; however, we prefer to keep Γ_j and B_j separate because they both have clear physical meanings (see Appendix B).

The imperfection of a quantum gate comes from imperfect control of the Hamiltonian $H(t)$ and from decoherence. If both imperfections are small, we can consider them separately. So, in this section we assume perfect $H(t)$ and analyze the process error matrix due to decoherence only. Moreover, we will consider only one decoherence mechanism, since summation over them is simple and can be done later. Therefore we will drop the index j in Eq. (62) and characterize the decoherence process by B and $\Gamma(t)$.

To find the error matrix χ^{err} (or $\tilde{\chi}^{\text{err}}$) of such operation, we can divide the total gate duration t_G into small timesteps Δt , for each of them representing the evolution as the desired unitary $\exp[-iH(t)\Delta t]$ and the error process $\chi^{\text{err}}(t, \Delta t)$. Then using the same idea as in section V, we can jump the error processes over the unitaries, moving them to the very end (for χ^{err}) or to the very beginning of the gate (for $\tilde{\chi}^{\text{err}}$). Finally, we can add up the error processes for all Δt using approximations (39)–(44).

For small Δt the error matrix $\chi^{\text{err}}(t, \Delta t)$ can be found by expanding B and $B^\dagger B$ in the Pauli basis, $B = \sum_n b_n E_n$, $B^\dagger B = \sum_n c_n E_n$, and then comparing the decoherence terms in Eq. (62) with Eq. (1),

$$\chi_{mn}^{\text{err}}(t, \Delta t) = \chi_{mn}^{\mathbf{I}} + \Gamma \Delta t \mathcal{B}_{mn}, \quad (63)$$

$$\mathcal{B}_{mn} = b_m b_n^* - \frac{1}{2}(c_m \delta_{n0} + c_n^* \delta_{m0}), \quad (64)$$

$$b_n = \frac{1}{d} \text{Tr}(B E_n^\dagger), \quad (65)$$

$$c_n = \frac{1}{d} \text{Tr}(B^\dagger B E_n^\dagger) = \frac{1}{d} \sum_{p,q} b_p^* b_q \text{Tr}(E_p^\dagger E_q E_n^\dagger). \quad (66)$$

It is easy to see that $c_n = c_n^*$ since $E_n^\dagger = E_n$ for the Pauli basis, so the left-column and top-row contributions due to the c -terms in Eq. (64) are real. Note that we can always use the transformation $B \rightarrow B - b_0 \mathbf{1}$ in the Lindblad equation, which compensates (zeroes) the component b_0 but changes the Hamiltonian, $H \rightarrow H + H_a$ with $H_a = i\hbar(\Gamma/2)(b_0^* B - b_0 B^\dagger)$ (there is no change, $H_a = 0$, if B is Hermitian). Therefore we can use $b_0 = 0$ in Eq. (64), and then the left-column and top-row elements come only from the c -terms, which correspond to the terms $-(B^\dagger B \rho - \rho B^\dagger B)/2$ of the Lindblad equation and so correspond to the “no-jump” evolution (see Appendix B).

Thus we have a clear physical picture of where the components of $\chi^{\text{err}}(t, \Delta t) - \chi^{\mathbf{I}}$ come from: the imaginary parts of the left-column and top-row elements come from the unitary imperfection (which may also be related to the decoherence-induced change of the Hamiltonian), the real parts of the left-column and top-row elements come from the “no-jump” evolution (see Appendix B), and other elements come from the decoherence “jumps”, which “strongly” change the state (recall that B have only components orthogonal to $\mathbf{1}$). A similar interpretation has been used in Sec. IV. Note that $\tilde{\chi}^{\text{err}}(t, \Delta t) = \chi^{\text{err}}(t, \Delta t)$ for small Δt because there is practically no unitary evolution.

Now let us use the language of $\tilde{\chi}^{\text{err}}$, which relates the error process to the beginning of the gate ($t = 0$). We can find $\tilde{\chi}^{\text{err}}$ by moving the error processes $\tilde{\chi}^{\text{err}}(t, \Delta t)$ to the start of the gate using the transformation relation (47) and then summing up the error contributions using the approximate additive rule (41). In this way we obtain

$$\tilde{\chi}^{\text{err}} \approx \chi^{\mathbf{I}} + \int_0^{t_G} \Gamma W^\dagger(t) \mathcal{B} W(t) dt, \quad (67)$$

$$W_{mn}(t) = \frac{1}{d} \text{Tr}[E_m^\dagger U(t) E_n U^\dagger(t)], \quad (68)$$

$$U(t) = \exp\left[\frac{-i}{\hbar} \int_0^t H(t) dt\right], \quad (69)$$

where \mathcal{B} is given by Eq. (64), $U(t)$ is the unitary evolution occurring within the interval $(0, t)$, and Eq. (69) assumes the time-ordering of operators.

Similar procedure can be used to find χ^{err} ; then we should move the errors to the end of the gate, by jumping

them over the remaining unitary $U_{\text{rem}}(t) = U(t_G)U^\dagger(t)$,

$$\chi^{\text{err}} \approx \chi^{\mathbf{I}} + \int_0^{t_G} \Gamma W_{\text{rem}}(t) \mathcal{B} W_{\text{rem}}^\dagger(t) dt, \quad (70)$$

$$W_{\text{rem},mn}(t) = \frac{1}{d} \text{Tr}[E_m^\dagger U(t_G)U^\dagger(t) E_n U(t)U^\dagger(t_G)]. \quad (71)$$

Note that the W_{rem} -transformation of \mathcal{B} in Eq. (70), $\mathcal{B}(t) \equiv W_{\text{rem}}(t) \mathcal{B} W_{\text{rem}}^\dagger(t)$, is equivalent to the U_{rem} -transformation of the Kraus operator B , which relates it to the end of the gate,

$$B(t) = U_{\text{rem}}(t) B U_{\text{rem}}^\dagger(t). \quad (72)$$

Therefore instead of Eq. (70) we can use

$$\chi^{\text{err}} \approx \chi^{\mathbf{I}} + \int \Gamma \mathcal{B}(t) dt, \quad (73)$$

in which $\mathcal{B}(t)$ is given by Eqs. (64)–(66) using $B(t)$ instead of B . Similarly, instead of Eq. (67) we can use

$$\tilde{\chi}^{\text{err}} \approx \chi^{\mathbf{I}} + \int \Gamma \tilde{\mathcal{B}}(t) dt, \quad (74)$$

in which $\tilde{\mathcal{B}}(t)$ is given by Eqs. (64)–(66) with

$$\tilde{B}(t) \equiv U^\dagger(t) B U(t) \quad (75)$$

instead of B . Note that if B is orthogonal to $\mathbf{1}$ ($b_0 = 0$, see discussion above), then $B(t)$ and $\tilde{B}(t)$ are also orthogonal to $\mathbf{1}$, so they still describe “strong” error jumps.

Since the element $\mathcal{B}_{00} = |b_0|^2 - c_0 = -\sum_{n \neq 0} |b_n|^2$ does not change in the transformation $W_{\text{rem}} \mathcal{B} W_{\text{rem}}^\dagger$, in the approximation (70) the fidelity is

$$F_\chi \approx 1 - \int_0^{t_G} \Gamma \sum_{n \neq 0} |b_n|^2 dt, \quad (76)$$

so that if Γ does not depend on time, then $F_\chi \approx 1 - t_G \Gamma \sum_{n \neq 0} |b_n|^2$ decays linearly with the gate time t_G . (As discussed above, the element b_0 is equivalent to a unitary imperfection, and therefore brings infidelity, which scales quadratically with time.) An interesting observation is that in this approximation the fidelity does not depend on the desired unitary evolution $U(t)$. Therefore, for example, for *any two-qubit gate* (which does not involve higher physical levels in the qubits) the contribution to the infidelity due to the energy relaxation and (Markovian non-correlated) pure dephasing of the qubits is

$$1 - F_\chi = \frac{t_G}{2T_1^{(a)}} + \frac{t_G}{2T_1^{(b)}} + \frac{t_G}{2T_\varphi^{(a)}} + \frac{t_G}{2T_\varphi^{(b)}}, \quad (77)$$

where T_1 is the energy relaxation time, T_φ is the pure dephasing time, and the qubits are labeled by superscripts (a) and (b) (see Appendix A). The independence of the fidelity (76) on the unitary evolution can be understood

in the following way. The process fidelity F_χ is related to the state fidelity, uniformly averaged over all pure initial states. A unitary evolution does not change the uniform distribution of pure states; therefore, the average rate of rare “decoherence jumps” does not depend on the unitary part.

The approximation (67)–(76) neglects the second-order corrections. In the case of significant coherent errors (which is not typical when only Lindblad-equation decoherence is discussed), the natural second-order correction is to add $\chi_{m0}^{\text{err}}(\chi_{0n}^{\text{err}})^*$ to the elements χ_{mn}^{err} with $m \neq 0$ and $n \neq 0$ (we assume $1 - F_\chi \ll 1$). Since this correction is small, it may be important only for the diagonal elements χ_{nn}^{err} , because it affects the resulting fidelity $F_\chi = 1 - \sum_{n \neq 0} \chi_{nn}^{\text{err}}$. This will introduce correction into Eq. (76), which scales quadratically with the gate time t_G . The similar second-order correction $\tilde{\chi}_{m0}^{\text{err}}(\tilde{\chi}_{0n}^{\text{err}})^*$ can be introduced to the elements of $\tilde{\chi}_{mn}^{\text{err}}$.

Note that in Eqs. (70) and (73) the elements of χ^{err} are linear in the decoherence rate Γ . Therefore the “pattern” of χ^{err} elements is determined by the decoherence mechanism characterized by the operator \mathcal{B} and its transformation $W_{\text{rem}}(t)$, and this pattern is multiplied by the decoherence rate Γ . (The experimental χ^{err} may need subtraction of the discussed above second-order correction to become linear in Γ .)

If there are several decoherence mechanisms in Eq. (62), then in the first order their contributions to χ^{err} simply add up. Therefore, if the patterns for the different decoherence mechanisms B_j are sufficiently simple and distinguishable from each other, then the decoherence rates Γ_j can be found directly from the experimentally measured χ^{err} (again, subtraction of the second-order correction may be useful in the case of significant coherent errors).

VIII. SPAM IDENTIFICATION

A very important difficulty in experimental implementation of the QPT is due to SPAM errors: imperfect preparation of the initial states and state tomography errors, which include imperfect tomographic single-qubit rotations and imperfect measurement of qubits. In this section we discuss a way, which may help solving this problem.

First, let us assume that the imperfect state preparation can be represented as an error channel, which acts on the ideal initial state. If we use 4^N initial states of N qubits, then the transformation between 4^N ideal and real density matrices of the initial states can always be described by a linear transformation, characterized by 16^N parameters. So by the number of parameters it seems that the representation of the preparation error by an error channel is always possible. The problem, however, is that this transformation may happen to be non-positive. Also, if more than 4^N initial states are used in an experiment, then an error-channel representation

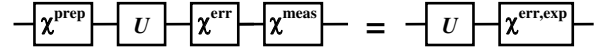


FIG. 3: Representation of the SPAM errors by the error processes χ^{prep} and χ^{err} .

may be impossible by the number of parameters. Nevertheless, we will use this representation, arguing that it can somehow be introduced phenomenologically. Similarly, we assume that the imperfections of the tomographic single-qubit rotations and measurement can also be represented as an error channel.

Using these two assumptions, we describe the preparation errors by the error matrix χ^{prep} (which is close to the ideal memory χ^{I}), and the tomography/measurement errors are described by χ^{meas} (also close to χ^{I}) – see Fig. 3. Thus the experimentally measured error matrix $\chi^{\text{err,exp}}$ is due to χ^{prep} , χ^{err} (which we need to find) and χ^{meas} .

The general idea is to measure χ^{prep} and χ^{meas} by doing the process tomography without the gate (doing the tomography immediately on the initial states) and then subtract this SPAM error from $\chi^{\text{err,exp}}$ to obtain χ^{err} . So, the procedure which first comes to mind is to use $\chi^{\text{err}} \approx \chi^{\text{err,exp}} - (\chi^{\text{err,I}} - \chi^{\text{I}})$, where $\chi^{\text{err,I}}$ is the experimentally measured χ without the gate. However, in general this would be wrong. The reason is that without the gate we measure the simple sum of the SPAM-error components [see Eq. (41)],

$$\chi^{\text{err,I}} \approx \chi^{\text{prep}} + \chi^{\text{meas}} - \chi^{\text{I}}, \quad (78)$$

but in the presence of the gate U the preparation error χ^{prep} changes because it is “jumped over” U [see Sec. V and Eq. (45)], so that

$$\chi^{\text{err,exp}} \approx \chi^{\text{err}} + W_{(U)}(\chi^{\text{prep}} - \chi^{\text{I}})W_{(U)}^\dagger + (\chi^{\text{meas}} - \chi^{\text{I}}), \quad (79)$$

where $W_{(U)}$ is given by Eq. (34). Therefore to find the actual error matrix χ^{err} from the experimental $\chi^{\text{err,exp}}$, it is insufficient to know $\chi^{\text{err,I}}$. We can still find χ^{err} from Eq. (79), but we need to know χ^{prep} and χ^{meas} separately.

The idea how to find both χ^{prep} and χ^{meas} is to do a calibration QPT with a set of gates with very high fidelity, for which the error is negligible, and then use Eq. (79) to separate the changing contribution from χ^{prep} and non-changing contribution from χ^{meas} . For example, in experiments with superconducting qubits the one-qubit π and $\pi/2$ rotations about X and Y axes usually have much better fidelity than two-qubit or multi-qubit gates. Therefore, for the QPT of a two-qubit or multi-qubit gate we can rely on the SPAM-error identification using these one-qubit gates.

Let us start with considering a single qubit and discussing the change $\chi^{\text{prep}} \rightarrow \chi_{(U)}^{\text{prep}} = W_{(U)}\chi^{\text{prep}}W_{(U)}^\dagger$ of the preparation error contribution, when we apply a high-fidelity X gate, $U = X$. By using Eq. (79) or by simply comparing the terms in the equation $\sum_{mn} \chi_{(X),mn}^{\text{prep}} E_m X \rho_{\text{in}} X E_n = \sum_{mn} \chi_{mn}^{\text{prep}} X E_m \rho_{\text{in}} E_n X$,

it is easy to find that this transformation flips the signs of the off-diagonal elements IY , IZ , XY , and XZ of χ^{prep} (the same for the symmetric, complex-conjugate elements), while the off-diagonal elements IX and YZ (and symmetric elements) do not change. The diagonal elements do not change, as expected for a Pauli twirling. Similarly, if we apply the high-fidelity Y gate, then the off-diagonal elements IX , IZ , XY , and YZ flip the sign, while the elements IY and XZ do not change. Recall that the contribution from χ^{meas} does not change. Therefore, by comparing $\chi^{\text{err,exp}}$ for the gates X , Y , and I (no gate), we can find separately all the off-diagonal elements of χ^{prep} and χ^{meas} .

To find diagonal elements of χ^{prep} and χ^{meas} , we can use high-fidelity gates \sqrt{X} ($\pi/2$ rotation over X axis) and \sqrt{Y} ($\pi/2$ rotation over Y axis). The gate \sqrt{X} exchanges diagonal elements YY and ZZ of χ^{prep} (it also exchanges and flips signs of some off-diagonal elements, but for simplicity we focus on the diagonal elements only). Similarly, the operation \sqrt{Y} exchanges the elements XX and ZZ of χ^{prep} . Since the elements of χ^{meas} do not change, we can find the diagonal elements of χ^{prep} and χ^{meas} separately. Actually, this cannot be done in the unique way, because the contributions proportional to $\mathbb{1}$ in $\chi^{\text{prep}} - \chi^{\text{I}}$ and in $\chi^{\text{meas}} - \chi^{\text{I}}$ are indistinguishable from each other (these are the depolarization-channel contributions). However, this non-uniqueness is not important because any choice gives the same SPAM-error contribution to $\chi^{\text{err,exp}}$.

In this way, by doing QPT of the gates X , Y , \sqrt{X} , \sqrt{Y} and I for a single qubit, we can find χ^{prep} and χ^{meas} (assuming that these gate are nearly perfect in comparison with preparation and measurement errors). For two or more qubits we can do the similar procedure, applying the combinations of these 5 single-qubit gates, and thus identifying all the elements of the multi-qubit matrices χ^{prep} and χ^{meas} . In fact, the system of equations for this identification is overdetermined, so we can either use an ad-hoc way of calculating the elements or use the numerically efficient least-square method (via the pseudo-inverse). Note that the described procedure has an obvious relation to the Pauli and Clifford twirling, but for us it is sufficient to use only a small subset of operations, and we do not average the result.

The described procedure of the SPAM-error identification [which is then subtracted from $\chi^{\text{err,exp}}$ using Eq. (79)] is surely very cumbersome. However, this is at least some way to deal with the SPAM problem, which does not seem to have a simple solution. Moreover, there are several ways to make experimental procedure less cumbersome, which are discussed next.

The situation is greatly simplified if the SPAM-error is dominated by only one component: either χ^{prep} or χ^{meas} . If χ^{prep} is negligible, then from Eq. (79) we see that the error matrix of the analyzed multi-qubit gate U can be estimated as

$$\chi^{\text{err}} \approx \chi^{\text{err,exp}} - (\chi^{\text{err,I}} - \chi^{\text{I}}), \quad (80)$$

so besides the standard QPT of the U gate we only need

the QPT of no operation (I gate). In the opposite limit when χ^{meas} is negligible, it is easier to use the language of $\tilde{\chi}^{\text{err}}$, because we can neglect the change of χ^{meas} when it is jumped over U to the left. In this case

$$\tilde{\chi}^{\text{err}} \approx \tilde{\chi}^{\text{err,exp}} - (\chi^{\text{err,I}} - \chi^{\text{I}}); \quad (81)$$

recall that $\tilde{\chi}^{\text{err,I}} = \chi^{\text{err,I}}$.

When both χ^{prep} and χ^{meas} are significant in the SPAM-error, it is still possible to simplify the described above procedure by using the idea of compressed-sensing QPT [35–37]. In contrast to the usual application of the compressed-sensing idea to the QPT of the gate U , we can apply it to find χ^{prep} and χ^{meas} by using a small random subset of 5^N combinations of single-qubit gates in the procedure. It is also possible to combine the random choice of the gates with the random choice of initial states and measurement directions, thus further reducing the amount of experimental work. It is important to emphasize that we do not need to know the matrices χ^{prep} and χ^{meas} very precisely, so their compressed-sensing estimate should be sufficient.

One more idea, which may be practically useful, is to measure $\chi^{\text{err,I}}$ and select only few significant peaks in it. For each of these peaks we identify which contribution to it comes from χ^{prep} and from χ^{meas} by applying just one or a few single-qubit rotations, which change this particular peak. It is beneficial to choose the rotations, which affect more than one significant peak of $\chi^{\text{err,I}}$. In this way a relatively small number of QPTs is sufficient to find the significant peaks of χ^{prep} and χ^{meas} . Then by using Eq. (79) we estimate the SPAM contribution for the multi-qubit gate U and subtract it from the experimental error matrix $\chi^{\text{err,exp}}$ to find “actual” χ^{err} .

Note that we do not need a complicated procedure to find the “actual” process fidelity F_χ of the gate U . If the SPAM errors can be represented by the error channels (Fig. 3) and if there are no significant coherent SPAM errors, then

$$F_\chi \approx F_\chi^{\text{exp}} / F_\chi^{\text{I}}, \quad (82)$$

where $F_\chi^{\text{exp}} = \chi_{00}^{\text{err,exp}}$ and $F_\chi^{\text{I}} = \chi_{00}^{\text{err,I}}$ are the experimentally measured fidelities for the gate U and no gate, respectively [see Eq. (44)].

IX. CONCLUSION

In this paper we have discussed representation of quantum operations via the error matrices. Instead of characterizing an operation by the standard process matrix χ , we separate the desired unitary operation U and the error process, which is placed either after or before U (Fig. 1). This defines two error matrices: χ^{err} and $\tilde{\chi}^{\text{err}}$ [Eqs. (8) and (9)]. We use the standard Pauli basis $\{E_n\}$ for all process matrices. The error matrices χ^{err} and $\tilde{\chi}^{\text{err}}$ are related to χ via unitary transformations [Eqs. (10) and (11)], as well as to each other [Eqs. (33) and (34)].

Therefore the error matrices are equivalent to χ ; however, they are more convenient to use than χ . The error matrices have only one large element, which is located at the top left corner and is equal to the process fidelity F_χ . Any other non-zero element corresponds to an imperfection of the quantum gate. Therefore, the bar chart of χ^{err} (or $\tilde{\chi}^{\text{err}}$) is a visually convenient way of representing the imperfections of an experimental quantum gate.

The elements of χ^{err} (or $\tilde{\chi}^{\text{err}}$) have more intuitive physical meaning related to the operation imperfection, than the elements of χ (even though the meaning of most of the elements is still not as intuitive as we would wish). It is important that since the error-matrix elements are small for a high-fidelity gate, the first-order approximation is typically sufficient. The imaginary parts of the elements in the left column and top row correspond to the unitary imperfection, $U^{\text{err}} \approx \mathbb{1} + \sum_{n>0} i \text{Im}(\chi_{n0}^{\text{err}}) E_n / F_\chi$, where the correction factor $1/F_\chi$ can be taken seriously only if most of infidelity comes from decoherence. The real parts of the elements in the left column and top row correspond to the small non-unitary change of the quantum state in the case when no “jumps” due to decoherence occur (this change is due to the Bayesian update, see Appendix B). It is natural to combine this non-unitary change with the unitary imperfection into a “coherent” (or “gradual”) state change, which happens in absence of “jumps”. Finally, other elements of χ_{mn}^{err} , with $m \neq 0$ and $n \neq 0$, correspond to the strong “jumps” of the quantum state due to decoherence. These jumps are characterized by Kraus operators practically orthogonal to $\mathbb{1}$ and therefore always bring an error (see discussions in Secs. IV and VII). The diagonal elements χ_{nn}^{err} with $n \neq 0$ (probabilities of E_n -type errors in the Pauli twirling approximation [46, 47]) have contributions from both the “coherent” imperfection and decoherence “jump” processes; however, the “coherent” contribution to χ_{nn}^{err} is of second order (crudely, $|\chi_{n0}^{\text{err}}|^2$ or $|\chi_{n0}^{\text{err}}|^2 / F_\chi$), so typically the main contribution is expected to be from decoherence, unless the unitary part is very inaccurate. We mainly discuss χ^{err} , but everything is practically the same in the language of $\tilde{\chi}^{\text{err}}$.

The composition of two error processes in the absence of desired unitary operations can be represented in the first order as a simple addition of the corresponding error matrices [Eqs. (39)–(41)]. However, if for M sequential error processes the “coherent” elements $\text{Im}(\chi_{n0}^{\text{err}})$ add up with the same phases and thus the sum grows linearly with M , then the second-order contribution (in particular, to the diagonal elements χ_{nn}^{err}) grows as M^2 , and for large M it can become significant in comparison with the first-order decoherence contribution, which grows linearly with M . For a composition of two quantum gates with non-trivial desired unitaries we need first to “jump” the error process over the unitary (see Fig. 2), that is described by the transformation (45), and then add the error matrices.

Essentially the same procedure can be done to calculate the error matrix contribution due to the Lindblad-

form decoherence in a quantum gate, which has finite duration and non-trivial evolution in time. For each short time step Δt the decoherence produces a contribution to χ^{err} [Eq. (63)], but this contribution should be “jumped over” the unitary evolution to the beginning or the end of the gate before being summed up [Eqs. (67) and (70)]. The equivalent language is to “jump” the decoherence Kraus operators over the desired unitaries, before the summation of error matrices [Eqs. (72)–(75)]. It is interesting that in the leading order the contribution to the infidelity $1 - F_\chi$ from the decoherence (if it occurs within the same Hilbert space) does not depend on the desired unitary evolution [Eqs. (76) and (77)].

Since the elements $\text{Im}(\chi_{n0}^{\text{err}})$ directly tell us about the unitary imperfection, it is easy to find the needed unitary correction [Eq. (49)] and the corresponding fidelity improvement [Eq. (50)]. However, the fidelity improvement is of second order and therefore is typically not expected to be significant. We have considered a particular example of correcting a CZ gate using single-qubit Z -rotations and CZ-phase corrections [Eqs. (58)–(61)].

The QPT suffers from errors in preparing the initial states and tomography measurement (SPAM errors). While this problem does not seem to have a simple solution, in Sec. VIII we have discussed a way, which may be helpful in alleviating this problem. A natural idea is to measure the error matrix $\chi^{\text{err},I}$ in the absence of the gate and then subtract it from the measured error matrix $\chi^{\text{err},\text{exp}}$ of the characterized gate U . However, this idea works only if the SPAM is dominated by one type of error: either at the preparation or at the tomography measurement. In general we need to know the contributions χ^{prep} and χ^{meas} from both errors separately because their addition depends on the gate U [Eq. (79)]. This can be done if some high-fidelity single-qubit gates are available; then analyzing the change of $\chi^{\text{err},\text{exp}}$ with application of different high-fidelity gates, we can separate the contributions from χ^{prep} and χ^{meas} . Note that this method assumes that the SPAM-errors can be represented as error processes at the preparation and tomography stages; the accuracy of this assumption is questionable. One of the ways to check this assumption is to check one of its predictions: Eq. (82) says that the “actual” fidelity of a quantum gate is the ratio of its QPT-measured fidelity and fidelity of the no-gate operation. The gate fidelity calculated in this way can then be compared with the fidelity obtained from the randomized benchmarking.

The appendices of this paper are to a significant extent separated from the main text. In Appendix A we consider several simple examples of χ -matrices for unitary evolution and decoherence, including the energy relaxation and pure dephasing (Markovian and non-Markovian). In Appendix B we discuss unraveling of the Lindblad-form evolution into the “jump” and “no-jump” scenarios, which can bring useful intuition in the analysis of decoherence; several examples are considered to illustrate the technique.

Reiterating the main point of this paper, we think that

characterization of quantum gates by error matrices in the Pauli basis is a convenient way of presenting experimental QPT results.

Acknowledgments

The author thanks Yuri Bogdanov, Abraham Kofman, Justin Dressel, Andrzej Veitia, Jay Gambetta, Michael Geller, and John Martinis for useful discussions. The research was funded by the Office of the Director of National Intelligence (ODNI), Intelligence Advanced Research Projects Activity (IARPA), through the Army Research Office Grant No. W911NF-10-1-0334. All statements of fact, opinion, or conclusions contained herein are those of the authors and should not be construed as representing the official views or policies of IARPA, the ODNI, or the U.S. Government. We also acknowledge support from the ARO MURI Grant No. W911NF-11-1-0268.

Appendix A: Simple examples of QPT

In this Appendix we consider several simple examples of the quantum processes, for which we calculate the standard process matrix χ of the QPT.

The matrix χ is defined via Eq. (1), which is copied here for convenience,

$$\rho_{\text{fin}} = \sum_{m,n} \chi_{mn} E_m \rho_{\text{in}} E_n^\dagger. \quad (\text{A1})$$

For the operator basis $\{E_n\}$ we use the Pauli basis, so that for one qubit it consists of four Pauli matrices,

$$I = \begin{pmatrix} 1 & 0 \\ 0 & 1 \end{pmatrix}, \quad X = \sigma_x = \begin{pmatrix} 0 & 1 \\ 1 & 0 \end{pmatrix}, \quad (\text{A2})$$

$$Y = \sigma_y = \begin{pmatrix} 0 & -i \\ i & 0 \end{pmatrix}, \quad Z = \sigma_z = \begin{pmatrix} 1 & 0 \\ 0 & -1 \end{pmatrix}, \quad (\text{A3})$$

while for several qubits the Kronecker (direct, outer, tensor) product of these matrices is used. We use the notation [1] in which $\alpha|0\rangle + \beta|1\rangle = \begin{pmatrix} \alpha \\ \beta \end{pmatrix}$.

1. Matrix χ for unitary operations

One-qubit rotations

As a very simple example, let us calculate the matrix χ for a Z -rotation of a qubit over the angle φ . This realizes the unitary operator U , which acts as $U(\alpha|0\rangle + \beta|1\rangle) = \alpha|0\rangle + \beta e^{i\varphi}|1\rangle$ (we use the sign convention of Ref. [1]). Then since $|\psi\rangle\langle\psi| \rightarrow U|\psi\rangle\langle\psi|U^\dagger$, we have in general $\rho_{\text{fin}} = U\rho_{\text{in}}U^\dagger$. Let us represent U in the Pauli basis,

$$U = \begin{pmatrix} 1 & 0 \\ 0 & e^{i\varphi} \end{pmatrix} = e^{i\varphi/2} \left(\cos\frac{\varphi}{2} I - i\sin\frac{\varphi}{2} Z \right), \quad (\text{A4})$$

where the unimportant overall phase factor $e^{i\varphi/2}$ does not affect the density matrix evolution, so that

$$\rho_{\text{fin}} = \left[\left(\cos\frac{\varphi}{2} I - i\sin\frac{\varphi}{2} Z \right) \rho_{\text{in}} \left(\cos\frac{\varphi}{2} I + i\sin\frac{\varphi}{2} Z \right) \right] \quad (\text{A5})$$

(note that the Pauli matrices are Hermitian, so we do not need to conjugate them). Now by comparing Eq. (A5) with Eq. (A1) we immediately find

$$\chi_{II} = \cos^2\frac{\varphi}{2}, \quad \chi_{ZZ} = \sin^2\frac{\varphi}{2}, \quad (\text{A6})$$

$$\chi_{IZ} = i\cos\frac{\varphi}{2}\sin\frac{\varphi}{2}, \quad \chi_{ZI} = -\chi_{IZ}, \quad (\text{A7})$$

other elements are zero. It is easy to see that the method of finding χ by comparing Eq. (A5) with Eq. (A1) is equivalent to using Eq. (4).

In a similar way we can calculate the matrix χ for a one-qubit X -rotation over angle φ . The result is obviously the same as Eqs. (A6)–(A7), with index Z replaced by X : $\chi_{II} = \cos^2(\varphi/2)$, $\chi_{XX} = \sin^2(\varphi/2)$, $\chi_{IX} = -\chi_{XI} = i(\cos\varphi)/2$. Similarly, for Y -rotations we replace Z in Eqs. (A6)–(A7) with Y .

A qubit rotation about an axis \vec{n} on the Bloch sphere over an angle φ corresponds to the unitary operator [1]

$$U = \exp[-i\frac{\varphi}{2}(\vec{n}\vec{\sigma})] = \left(\cos\frac{\varphi}{2} I - i\sin\frac{\varphi}{2} (\vec{n}\vec{\sigma}) \right), \quad (\text{A8})$$

where $\vec{n}\vec{\sigma} \equiv n_x\sigma_x + n_y\sigma_y + n_z\sigma_z$. Note that this formula neglects the overall phase factor (which does not exist in the Bloch-sphere space), as seen by comparing it with Eq. (A4). Using Eq. (4) or, alternatively, comparing equation $\rho_{\text{fin}} = U\rho_{\text{in}}U^\dagger$ with the definition (A1), we still can easily find the elements of the χ -matrix; now all 16 elements are in general non-zero, though they are determined by only 3 real parameters.

Two-qubit unitaries

Let us start with the case when the first qubit is Z -rotated over the angle φ , while the second qubit is “idling”. Then the unitary operator is $U = [(\cos\frac{\varphi}{2})I - i(\sin\frac{\varphi}{2})Z] \otimes I$, and Eq. (A5) becomes

$$\rho_{\text{fin}} = [(\cos I - i\sin Z) \otimes I] \rho_{\text{in}} [(\cos I + i\sin Z) \otimes I], \quad (\text{A9})$$

where for brevity we omit the argument $\varphi/2$ of sines and cosines. Comparing this equation with (A1), we have to use double-letter combinations for both indices m and n ; however, we see that the second-qubit letter is always I , so we essentially obtain the single-qubit result (A6)–(A7) with added index I for the second qubit:

$$\chi_{II,II} = \cos^2(\varphi/2), \quad \chi_{ZI,ZI} = \sin^2(\varphi/2), \quad (\text{A10})$$

$$\chi_{II,ZI} = -\chi_{ZI,II} = i\cos(\varphi/2)\sin(\varphi/2). \quad (\text{A11})$$

As another example, let us consider the controlled-phase operation (note that our use of the name

“controlled-phase” is different from the terminology of Ref. [1]),

$$U = \text{diag}(1, 1, 1, e^{i\theta}) = b(-ZZ + IZ + ZI) + cII, \quad (\text{A12})$$

$$b = (1 - e^{i\theta})/4, \quad c = (3 + e^{i\theta})/4, \quad (\text{A13})$$

where in this (rather sloppy) notation we omit the Kronecker product sign “ \otimes ”. By comparing $U\rho_{\text{in}}U^\dagger$ with (A1) we obtain 16 non-zero elements:

$$\chi_{II,II} = |c|^2, \quad \chi_{ZZ,ZZ} = \chi_{IZ,IZ} = \chi_{ZI,ZI} = |b|^2, \quad (\text{A14})$$

$$\chi_{IZ,ZI} = \chi_{ZI,IZ} = |b|^2, \quad (\text{A15})$$

$$\chi_{IZ,II} = \chi_{ZI,II} = bc^*, \quad \chi_{II,IZ} = \chi_{II,ZI} = b^*c, \quad (\text{A16})$$

$$\chi_{ZZ,IZ} = \chi_{ZZ,ZI} = \chi_{IZ,ZZ} = \chi_{ZI,ZZ} = -|b|^2, \quad (\text{A17})$$

$$\chi_{ZZ,II} = -bc^*, \quad \chi_{II,ZZ} = -b^*c. \quad (\text{A18})$$

The controlled-phase gate becomes the CZ gate at $\theta = \pi$. Then $b = c = 1/2$, and all 16 elements of χ in Eqs. (A14)–(A18) become $\pm 1/4$. Note that if in an experimental realization the phase θ fluctuates symmetrically around π with a small variance $\langle(\delta\theta)^2\rangle$, then the element $\chi_{II,II}$ increases by $(3/16)\langle(\delta\theta)^2\rangle$, while other 15 elements decrease in absolute value by $(1/16)\langle(\delta\theta)^2\rangle$.

For the perfect CNOT gate (with the first qubit being the control) the unitary can be represented as

$$U = \frac{I+Z}{2} \otimes I + \frac{I-Z}{2} \otimes X, \quad (\text{A19})$$

where we used the relations $(I+Z)/2 = |0\rangle\langle 0|$ and $(I-Z)/2 = |1\rangle\langle 1|$ (here we again use the notation “ \otimes ” for more clarity). Then non-zero elements of χ are

$$\chi_{II,II} = \chi_{IX,IX} = \chi_{ZI,ZI} = \chi_{ZX,ZX} = 1/4, \quad (\text{A20})$$

$$\chi_{II,IX} = \chi_{II,ZI} = \chi_{IX,II} = \chi_{ZI,II} = 1/4, \quad (\text{A21})$$

$$\chi_{II,ZX} = \chi_{ZX,II} = -1/4, \quad \chi_{IX,ZI} = \chi_{ZI,IX} = 1/4, \quad (\text{A22})$$

$$\chi_{IX,ZX} = \chi_{ZI,ZX} = \chi_{ZX,IX} = \chi_{ZX,ZI} = -1/4, \quad (\text{A23})$$

as directly follows from the combinations of 4 terms in Eq. (A19).

For the perfect $\sqrt{i\text{SWAP}}$ gate the unitary is

$$U = |00\rangle\langle 00| + |11\rangle\langle 11| - i(|01\rangle\langle 10| + |10\rangle\langle 01|) \quad (\text{A24})$$

$$= \frac{2 + \sqrt{2}}{4} II + \frac{2 - \sqrt{2}}{4} ZZ - \frac{i\sqrt{2}}{4} (XX + YY), \quad (\text{A25})$$

so the non-zero elements of the matrix χ are given by the pairwise products of these 4 terms,

$$\chi_{II,II} = (3 + 2\sqrt{2})/8, \quad \chi_{ZZ,ZZ} = (3 - 2\sqrt{2})/8, \quad (\text{A26})$$

$$\chi_{XX,XX} = \chi_{YY,YY} = 1/8, \quad (\text{A27})$$

$$\chi_{XX,YY} = \chi_{YY,XX} = \chi_{II,ZZ} = \chi_{ZZ,II} = 1/8, \quad (\text{A28})$$

$$\begin{aligned} \chi_{II,XX} &= \chi_{II,YY} = -\chi_{XX,II} = -\chi_{YY,II} \\ &= i(\sqrt{2} + 1)/8, \end{aligned} \quad (\text{A29})$$

$$\begin{aligned} \chi_{ZZ,XX} &= \chi_{ZZ,YY} = -\chi_{XX,ZZ} = -\chi_{YY,ZZ} \\ &= i(\sqrt{2} - 1)/8. \end{aligned} \quad (\text{A30})$$

2. One-qubit decoherence

Pure dephasing (exponential and non-exponential)

It is very easy to find the matrix χ for one qubit with pure dephasing (assuming no other evolution). After waiting for time t , the qubit is Z -rotated over a random angle φ . From the definition (A1) we see that for a random evolution we simply need to average the χ -matrix over the possible evolution realizations. Therefore the χ -matrix for pure dephasing is given by averaging Eqs. (A6)–(A7):

$$\chi_{ZZ} = \langle \sin^2 \frac{\varphi}{2} \rangle = \frac{1 - \langle \cos \varphi \rangle}{2}, \quad \chi_{II} = 1 - \chi_{ZZ}, \quad (\text{A31})$$

$$\chi_{IZ} = -\chi_{ZI} = i \langle \sin \varphi \rangle / 2, \quad (\text{A32})$$

where $\langle \dots \rangle$ denotes averaging over realizations. For a symmetric probability density distribution of φ we get $\langle \sin \varphi \rangle = 0$ and therefore $\chi_{IZ} = \chi_{ZI} = 0$, so the only non-zero elements are χ_{II} and χ_{ZZ} .

It is important to emphasize that the result (A31) does not assume exponential dephasing; it remains valid for an “inhomogeneous” contribution to the dephasing (slightly different qubit frequencies in different experimental runs) and/or the “1/f” contribution (when the qubit frequency fluctuation has a broad range of timescales). It is also important that the value $\langle \cos \phi \rangle$ which determines χ_{ZZ} can be directly obtained from the Ramsey-fringes data.

Let us consider the Ramsey protocol: start with $|0\rangle$, apply $\pi/2$ X -rotation, wait time t , apply the second $\pi/2$ rotation about the axis, which is shifted from X by an angle ϕ_R in the equatorial plane of the Bloch sphere, and finally measure the probability $P(|1\rangle)$ of the state $|1\rangle$. It is easy to find that for a pure dephasing (including non-exponential case)

$$P(|1\rangle) = \frac{1}{2} + \frac{\langle \cos(\phi_R + \varphi) \rangle}{2} = \frac{1}{2} + \frac{\langle \cos \varphi \rangle \cos \phi_R}{2}, \quad (\text{A33})$$

where for the second equation we assumed $\langle \sin \varphi \rangle = 0$. In the case of exponential dephasing characterized by the dephasing time T_φ , we have $\langle \cos \varphi \rangle = \exp(-t/T_\varphi)$. In the general case the time dependence of $\langle \cos \varphi \rangle$ is arbitrary; however, it can be found experimentally from the amplitude of the Ramsey oscillations and then can be used in Eq. (A31) to obtain χ_{ZZ} .

It is important to mention that experimentally T_φ is often defined as the time at which $\langle \cos \varphi \rangle = e^{-1}$. If the qubit dephasing is due to fast (“white noise”) fluctuations of the qubit energy, then $\langle \cos \varphi \rangle = e^{-t/T_\varphi}$ and correspondingly $\chi_{ZZ} = (1 - e^{-t/T_\varphi})/2$, so that at short time, $t \ll T_\varphi$, there is a linear dependence,

$$\chi_{ZZ} \approx t/2T_\varphi. \quad (\text{A34})$$

However, if the pure dephasing is dominated by the very slow fluctuations of the qubit energy, then $\langle \cos \varphi \rangle = \exp[-(t/T_\varphi)^2]$ and the Ramsey-fringes dependence has

a Gaussian shape. In this case at $t \ll T_\varphi$ the dephasing error is quadratic in time,

$$\chi_{ZZ} \approx t^2/2T_\varphi^2. \quad (\text{A35})$$

In the presence of both mechanisms

$$\langle \cos \varphi \rangle = \exp(-t/T_{\varphi,\text{fast}}) \exp[-(t/T_{\varphi,\text{slow}})^2]; \quad (\text{A36})$$

this formula can also be used as an approximation in the case of a broad range of the fluctuation timescales. The corresponding χ_{ZZ} is still given by Eq. (A31).

Note that in the presence of energy relaxation (discussed later) the value of $\langle \cos \varphi \rangle$ can still be directly extracted from the Ramsey-fringes data – see Eq. (A59) below.

Energy relaxation

Now let us calculate the matrix χ taking into account the qubit energy relaxation, but assuming the absence of pure dephasing. Let us start with the zero-temperature case (relaxation to the state $|0\rangle$ only). Using “unraveling” of the energy relaxation in the same way as in Refs. [55] and [56] (see also Appendix B), we may think about two probabilistic scenarios:

$$\alpha|0\rangle + \beta|1\rangle \rightarrow \begin{cases} |0\rangle \text{ with prob. } P_r = |\beta|^2(1 - e^{-t/T_1}) \\ \frac{\alpha|0\rangle + \beta e^{-t/2T_1}|1\rangle}{\sqrt{|\alpha|^2 + |\beta|^2 e^{-t/T_1}}} \text{ with prob. } 1 - P_r \end{cases} \quad (\text{A37})$$

(in the case of no relaxation the state evolves due to the Bayesian update). This corresponds to the technique of Kraus operators and for the density matrix gives

$$\rho_{\text{in}} \rightarrow A_r \rho_{\text{in}} A_r^\dagger + A_{no} \rho_{\text{in}} A_{no}^\dagger, \quad (\text{A38})$$

where the Kraus operators A_r (for the scenario with relaxation) and A_{no} (for the scenario with no relaxation) are

$$A_r = \begin{pmatrix} 0 & \sqrt{1 - e^{-t/T_1}} \\ 0 & 0 \end{pmatrix}, \quad A_{no} = \begin{pmatrix} 1 & 0 \\ 0 & e^{-t/2T_1} \end{pmatrix}. \quad (\text{A39})$$

Note that $A_r^\dagger A_r + A_{no}^\dagger A_{no} = \mathbb{1}$ (the completeness relation). Here we use the standard Kraus-operator representation [1, 51], in contrast to the somewhat modified representation (19).

To find the χ -matrix, we expand the Kraus operators in the Pauli basis,

$$A_r = \sqrt{1 - e^{-t/T_1}} \frac{X + iY}{2}, \quad (\text{A40})$$

$$A_{no} = \frac{1 + e^{-t/2T_1}}{2} I + \frac{1 - e^{-t/2T_1}}{2} Z. \quad (\text{A41})$$

Now comparing evolution (A38) with the form (A1), we collect the χ -matrix elements (the relaxation term brings

elements involving X and Y , while the no-relaxation term brings elements with I and Z):

$$\chi_{XX} = \chi_{YY} = (1 - e^{-t/T_1})/4, \quad (\text{A42})$$

$$\chi_{XY} = -\chi_{YX} = -i(1 - e^{-t/T_1})/4, \quad (\text{A43})$$

$$\chi_{II} = (1 + e^{-t/2T_1})^2/4, \quad \chi_{ZZ} = (1 - e^{-t/2T_1})^2/4, \quad (\text{A44})$$

$$\chi_{IZ} = \chi_{ZI} = (1 - e^{-t/T_1})/4. \quad (\text{A45})$$

Note that at small t/T_1 the element χ_{ZZ} is quadratic in time (very small), while other elements (except χ_{II}) are linear in time (in this case $\chi_{ZZ} \approx |\chi_{IZ}|^2$, as expected from the discussion in Sec. IV). Also note that the non-zero elements in the left column and top row (χ_{IZ} and χ_{ZI}) are real and come from the no-relaxation scenario (see Sec. IV).

For a non-zero temperature there are two kinds of the relaxation processes (up and down) with the rates Γ_\uparrow and Γ_\downarrow satisfying the standard relations $\Gamma_\uparrow + \Gamma_\downarrow = 1/T_1$ and $\Gamma_\uparrow/\Gamma_\downarrow = \exp(-E/T)$, where T is temperature and $E = E_1 - E_0$ is the energy difference between the qubit states; this gives $\Gamma_{\uparrow,\downarrow}^{-1} = T_1(1 + e^{\pm E/T})$. Correspondingly, there are three scenarios with the Kraus operators

$$A_{r\downarrow} = \begin{pmatrix} 0 & \sqrt{1 - e^{-\Gamma_\downarrow t}} \\ 0 & 0 \end{pmatrix}, \quad A_{r\uparrow} = \begin{pmatrix} 0 & 0 \\ \sqrt{1 - e^{-\Gamma_\uparrow t}} & 0 \end{pmatrix} \quad (\text{A46})$$

$$A_{no} = \begin{pmatrix} e^{-\Gamma_\uparrow t/2} & 0 \\ 0 & e^{-\Gamma_\downarrow t/2} \end{pmatrix}. \quad (\text{A47})$$

Then in a similar way as above we find the χ -matrix elements:

$$\chi_{XX} = \chi_{YY} = (1 - e^{-\Gamma_\downarrow t})/4 + (1 - e^{-\Gamma_\uparrow t})/4, \quad (\text{A48})$$

$$\chi_{XY} = -\chi_{YX} = -i(e^{-\Gamma_\uparrow t} - e^{-\Gamma_\downarrow t})/4, \quad (\text{A49})$$

$$\chi_{II} = (e^{-\Gamma_\uparrow t/2} + e^{-\Gamma_\downarrow t/2})^2/4, \quad (\text{A50})$$

$$\chi_{ZZ} = (e^{-\Gamma_\uparrow t/2} - e^{-\Gamma_\downarrow t/2})^2/4, \quad (\text{A51})$$

$$\chi_{IZ} = \chi_{ZI} = (e^{-\Gamma_\uparrow t} - e^{-\Gamma_\downarrow t})/4. \quad (\text{A52})$$

Pure dephasing combined with energy relaxation

Phase evolution commutes with the energy relaxation, therefore we may apply Z -rotation over a random angle φ after the energy relaxation. The Z -rotation does not affect scenario(s) with relaxation, so we need to change only the Kraus operator for the no-relaxation scenario: $A_{no} \rightarrow (I \cos \frac{\varphi}{2} - iZ \sin \frac{\varphi}{2})A_{no}$, then calculate the corresponding elements of the χ -matrix in the same way as above and average over φ . Therefore, the elements χ_{XX} , χ_{YY} , χ_{XY} , χ_{YX} due to energy relaxation will not be affected by the pure dephasing (since they come from the relaxation scenario). The calculation shows that the elements χ_{IZ} and χ_{ZI} are also not affected when $\langle \sin \varphi \cos \varphi \rangle = 0$ (satisfied for a symmetric noise), so the only affected elements are χ_{ZZ} and χ_{II} , which are non-zero for both decoherence mechanisms. Using again the

condition $\langle \sin \varphi \cos \varphi \rangle = 0$, it is easy to find

$$\chi_{ZZ} = \chi_{ZZ}^{deph} \chi_{II}^{rel} + \chi_{ZZ}^{rel} \chi_{II}^{deph}, \quad (\text{A53})$$

$$\chi_{II} = \chi_{II}^{deph} \chi_{II}^{rel} + \chi_{ZZ}^{deph} \chi_{ZZ}^{rel}, \quad (\text{A54})$$

where χ^{deph} and χ^{rel} correspond to pure dephasing and energy relaxation, and were calculated above [Eqs. (A31) and (A48)–(A52)]. For completeness let us also show the unaffected elements:

$$\chi_{XX} = \chi_{YY} = \chi_{XX}^{rel}, \quad \chi_{XY} = -\chi_{YX} = \chi_{XY}^{rel}, \quad (\text{A55})$$

$$\chi_{IZ} = \chi_{ZI} = \chi_{IZ}^{rel}. \quad (\text{A56})$$

Another way of deriving Eqs. (A53)–(A56) is the following. Let us apply pure dephasing after energy relaxation and write the composition of quantum operations as

$$\rho_{\text{fin}} = \sum_{m,n} \sum_{m',n'} \chi_{mn}^{rel} \chi_{m'n'}^{deph} E_{m'} E_m \rho_{\text{in}} E_n^\dagger E_{n'}^\dagger. \quad (\text{A57})$$

Even though a product of Pauli matrices is a Pauli matrix (possibly with a phase factor) and therefore χ -matrix of a composition of operations can in principle be calculated in a straightforward way, usually this is a very cumbersome procedure. However, in our case the matrix χ^{deph} has only two non-zero elements (χ_{II}^{deph} and χ_{ZZ}^{deph}), so the calculation is not very long and leads to Eqs. (A53)–(A56).

Now when we have explicit formulas for the χ -matrix elements, which depend on t/T_1 , temperature, and $\langle \cos \varphi \rangle$, let us discuss again how to extract $\langle \cos \varphi \rangle$ from the Ramsey-fringes data. In the presence of energy relaxation (at arbitrary temperature) the Ramsey oscillations are

$$P(|1\rangle) = \frac{1}{2} + \frac{e^{-(\Gamma_\downarrow + \Gamma_\uparrow)t/2}}{2} \langle \cos(\phi_R + \varphi) \rangle \quad (\text{A58})$$

$$= \frac{1}{2} + \frac{1}{2} e^{-t/2T_1} \langle \cos \varphi \rangle \cos \phi_R. \quad (\text{A59})$$

Therefore, if the energy relaxation time T_1 is measured separately, the Ramsey data give the value of $\langle \cos \varphi \rangle$ at any time t . This value can be used to calculate the χ -matrix even in the case of arbitrary non-exponential dephasing.

Now let us discuss the χ -matrix at a relatively short time t and neglect the terms quadratic in time. Then we obtain

$$\chi_{XX} = \chi_{YY} = t/4T_1, \quad \chi_{ZZ} = (1 - \langle \cos \varphi \rangle)/2, \quad (\text{A60})$$

$$\chi_{II} = 1 - t/2T_1 - (1 - \langle \cos \varphi \rangle)/2, \quad (\text{A61})$$

$$\chi_{XY} = -\chi_{YX} = -i(t/4T_1) \tanh(E/2T), \quad (\text{A62})$$

$$\chi_{IZ} = \chi_{ZI} = (t/4T_1) \tanh(E/2T). \quad (\text{A63})$$

In the case of exponential pure dephasing $\langle \cos \varphi \rangle = \exp(-t/T_\varphi)$, and then $\chi_{ZZ} = t/2T_\varphi$, where $T_\varphi^{-1} = T_2^{-1} - (2T_1)^{-1}$ and T_2 is the dephasing time.

Appendix B: Interpretation of the Lindblad-form master equation

In this Appendix we discuss the technique of Kraus operators applied to the evolution described by the standard Lindblad-form master equation. We show that each Lindblad term describes two evolutions: a “jump” process with some rate and a continuous evolution between the jumps caused by the absence of jumps. Such interpretation can be useful in intuitive analysis of decoherence processes.

A Markovian evolution of a quantum system is usually described by the Lindblad-form master equation [for convenience we copy Eq. (62) here]

$$\dot{\rho} = -\frac{i}{\hbar} [H, \rho] + \sum_n \Gamma_n (B_n \rho B_n^\dagger - \frac{1}{2} B_n^\dagger B_n \rho - \frac{1}{2} \rho B_n^\dagger B_n), \quad (\text{B1})$$

where the first term describes the unitary evolution due to the Hamiltonian H , while the n th decoherence mechanism is described by the “rate” Γ_n (real number with dimension s^{-1}) and dimensionless operator B_n . Note that mathematically Γ_n can be absorbed by redefining $\tilde{B}_n = \sqrt{\Gamma_n} B_n$; however, we do not do this because Γ_n and B_n have separate physical meanings.

Our goal here is to discuss a simple physical interpretation of the decoherence terms in the Lindblad equation ($H = 0$) and consider first only one decoherence mechanism; then we can omit the index n (summation over n is simple).

It is easy to check that the term $\Gamma B \rho B^\dagger$ corresponds to the abrupt change (“jump”) of the state

$$|\psi\rangle \rightarrow \frac{B|\psi\rangle}{\text{Norm}} = \frac{B|\psi\rangle}{\|B|\psi\rangle\|}, \quad \rho \rightarrow \frac{B\rho B^\dagger}{\text{Norm}} = \frac{B\rho B^\dagger}{\text{Tr}(B\rho B^\dagger)}, \quad (\text{B2})$$

which occurs with the rate (jump probability per second)

$$\frac{dP}{dt} = \Gamma \|B|\psi\rangle\|^2, \quad \frac{dP}{dt} = \Gamma \text{Tr}(B\rho B^\dagger) = \Gamma \text{Tr}(B^\dagger B \rho). \quad (\text{B3})$$

(Here we show the formulas in both the wavefunction and density matrix languages; the wavefunction language is usually more convenient to use.) Note a possible confusion in terminology: both Γ and dP/dt are rates; to distinguish them let us call Γ the “process rate” or just “rate”, while dP/dt will be called “jump rate”.

The remaining term $-(\Gamma/2)(B^\dagger B \rho + \rho B^\dagger B)$ in the Lindblad form corresponds to the jump process (B2) *not happening*. The physical reason of this evolution “when nothing happens” is the same as the partial collapse in the null-result measurement [48, 50]: this is essentially the Bayesian update [49], which accounts for the information that the jump did not happen. Therefore, *the physical meaning of the Lindblad form is the description of two scenarios: the jump process either happening or not happening*.

To see this mathematically, let us use the technique of Kraus operators [1, 51], in which the evolution $\rho_{\text{in}} \rightarrow \rho_{\text{fin}}$ is unraveled into the probabilistic mixture of “scenarios” described by Kraus operators A_k ,

$$|\psi_{\text{in}}\rangle \rightarrow \frac{A_k|\psi_{\text{in}}\rangle}{\text{Norm}}, \quad \rho_{\text{in}} \rightarrow \frac{A_k\rho_{\text{in}}A_k^\dagger}{\text{Norm}}, \quad (\text{B4})$$

with probabilities $P_k = \text{Tr}(A_k^\dagger A_k \rho_{\text{in}})$ [in the wavefunction language $P_k = \|A_k|\psi_{\text{in}}\rangle\|^2 = \text{Tr}(A_k^\dagger A_k |\psi_{\text{in}}\rangle\langle\psi_{\text{in}}|)$]. The sum of the probabilities should be equal to 1, which leads to the completeness relation

$$\sum_k A_k^\dagger A_k = \mathbb{1}. \quad (\text{B5})$$

Note the change of notations compared with Eq. (19).

During a short time Δt the evolution (B1) can be described by two scenarios: the jump either occurs or not, with the corresponding Kraus operators A_{jump} and A_{no} . For the jump scenario

$$A_{\text{jump}} = \sqrt{\Gamma\Delta t} B, \quad (\text{B6})$$

so that $A_{\text{jump}}\rho A_{\text{jump}}^\dagger = (\Gamma\Delta t)B\rho B^\dagger$ gives the same contribution to $\Delta\rho = \rho(t + \Delta t) - \rho(t)$ as the term $\Gamma B\rho B^\dagger$ in Eq. (B1). The no-jump Kraus operator A_{no} should satisfy the completeness relation (B5), $A_{\text{jump}}^\dagger A_{\text{jump}} + A_{\text{no}}^\dagger A_{\text{no}} = \mathbb{1}$. Using the Bayesian-update approach [49] in which $A_{\text{no}}^\dagger = A_{\text{no}}$, we find

$$A_{\text{no}} = \sqrt{\mathbb{1} - A_{\text{jump}}^\dagger A_{\text{jump}}} \approx \mathbb{1} - \frac{1}{2} A_{\text{jump}}^\dagger A_{\text{jump}} \quad (\text{B7})$$

$$= \mathbb{1} - \frac{1}{2} \Gamma\Delta t B^\dagger B. \quad (\text{B8})$$

Note that $A_{\text{jump}}^\dagger A_{\text{jump}}$ is a positive Hermitian operator and $\mathbb{1} - A_{\text{jump}}^\dagger A_{\text{jump}}$ is also a positive operator. A square root of a positive operator is defined via taking square roots of its eigenvalues in the diagonalizing basis. This is why in Eq. (B7) we deal with operators essentially as with numbers.

Using Eq. (B8) for A_{no} , we find in the linear order

$$A_{\text{no}}\rho A_{\text{no}}^\dagger \approx \rho - \frac{1}{2} \Gamma\Delta t B^\dagger B \rho - \frac{1}{2} \Gamma\Delta t \rho B^\dagger B, \quad (\text{B9})$$

with this linear-order approximation becoming exact at $\Delta t \rightarrow 0$. It is easy to see that Eq. (B9) gives the evolution described by the term $-(\Gamma/2)(B^\dagger B\rho + \rho B^\dagger B)$ in the Lindblad form (B1).

Thus we have shown that the Lindblad-form master equation (B1) with one decoherence term describes a jump process B [see Eq. (B2)] occurring with the jump rate (probability per second) $\Gamma \text{Tr}(B\rho B^\dagger)$. In the case of several decoherence mechanisms there are several Kraus operators $A_{n,\text{jump}} = \sqrt{\Gamma_n\Delta t} B_n$ describing the jumps $|\psi\rangle \rightarrow B_n|\psi\rangle/\text{Norm}$ during a short duration Δt . The no-jump Kraus operator in this case is $A_{\text{no}} =$

$\sqrt{\mathbb{1} - \sum_n (A_{n,\text{jump}}^\dagger A_{n,\text{jump}})} \approx \mathbb{1} - \sum_n (\frac{1}{2}\Gamma_n\Delta t B_n^\dagger B_n)$, which contributes to all terms $-(\Gamma_n/2)(B_n^\dagger B_n\rho + \rho B_n^\dagger B_n)$ in Eq. (B1).

Note that Eq. (B7) and its generalization for several processes is not the unique form for A_{no} , which follows from the completeness relation (B5). It is formally possible to add an arbitrary unitary rotation U , so that

$A_{\text{no}} = U\sqrt{\mathbb{1} - \sum_n (A_{n,\text{jump}}^\dagger A_{n,\text{jump}})}$, which does not affect $A_{\text{no}}^\dagger A_{\text{no}}$. Using a natural assumption that $U \rightarrow \mathbb{1}$ at $\Delta t \rightarrow 0$, we can expand U in the linear order as $U = \mathbb{1} - iH_a\Delta t$, where H_a should be a Hermitian matrix. Then $A_{\text{no}}\rho A_{\text{no}}^\dagger$ acquires the extra term $-i[H_a, \rho]\Delta t$, from which we see that H_a is essentially an addition to the Hamiltonian H . So the formalism permits a change of the Hamiltonian due to decoherence, and therefore H in Eq. (B1) should be considered as the effective Hamiltonian (which may include the “Lamb shift” mechanism).

Now let us consider several examples of decoherence processes in the language of “jumps”.

1. Energy relaxation of a qubit

For a qubit relaxation from the excited state $|1\rangle$ to the ground state $|0\rangle$ with the rate $\Gamma = 1/T_1$, the jump operator is $B = \begin{pmatrix} 0 & 1 \\ 0 & 0 \end{pmatrix}$, where the ground state corresponds to the upper line, so that $B|1\rangle = |0\rangle$, $B|0\rangle = 0$. In this case $B^\dagger B = \begin{pmatrix} 0 & 0 \\ 0 & 1 \end{pmatrix}$, so that the no-jump evolution during time Δt changes the qubit state as

$$\alpha|0\rangle + \beta|1\rangle \rightarrow \frac{\alpha|0\rangle + \beta e^{-\Delta t/2T_1}|1\rangle}{\text{Norm}} \approx \frac{\alpha|0\rangle + \beta(1 - \frac{\Delta t}{2T_1})|1\rangle}{\text{Norm}} \quad (\text{B10})$$

while in the case of jump obviously $\alpha|0\rangle + \beta|1\rangle \rightarrow |0\rangle$ (the jump rate is $\Gamma|\beta|^2$). These two evolutions give correct density matrix, which also follows from the Lindblad equation solution (see Sec. IIA of Ref. [56] for more detailed discussion).

The excitation processes $|0\rangle \rightarrow |1\rangle$ can be taken into account in the similar way using an additional Lindblad-form term.

2. Pure dephasing of a qubit

The physical mechanism of the Markovian pure dephasing in superconducting qubits is the fast (“white noise”) fluctuations of the qubit energy, which leads to random fluctuations of the qubit phase $\varphi = \arg(\alpha^*\beta) = \arg(\rho_{01})$, so that the random phase shift $\Delta\varphi$ accumulated during a short time Δt has the Gaussian probability distribution with zero mean and variance $(\Delta\varphi)^2 = 2\Delta t/T_\varphi$, where T_φ is the dephasing time.

It is easy to check that the correct evolution due to pure dephasing $[\rho_{01}(t) = \rho_{01}(0) e^{-t/T_\varphi}$, $\rho_{00}(t) = \rho_{00}(0)$,

$\rho_{11}(t) = \rho_{11}(0)$] can be reproduced using the Lindblad equation (B1) with $\Gamma = 1/2T_\varphi$ and $B = \begin{pmatrix} 1 & 0 \\ 0 & -1 \end{pmatrix}$. This means that instead of the physically correct picture of continuous change of φ , we may use a completely different picture: random jumps of the phase φ by π ,

$$\alpha|0\rangle + \beta|1\rangle \rightarrow \alpha|0\rangle - \beta|1\rangle, \quad (\text{B11})$$

occurring with the jump rate [see Eq. (B3)] $\Gamma \text{Tr}(B^\dagger B \rho) = 1/2T_\varphi$, which in this case is independent of the qubit state and equal to Γ . Note that $B^\dagger B = \mathbb{1}$, so in this case there is no no-jump evolution.

Since both pictures lead to the same evolution of $\rho(t)$, we can use any of them, depending on convenience in a particular problem. One more picture which can be used for pure dephasing is the “random measurement of state $|0\rangle$ ”, for which $B = \begin{pmatrix} 1 & 0 \\ 0 & 0 \end{pmatrix}$ and $\Gamma = 2/T_\varphi$. It is easy to see that it leads to the same Lindblad equation, but has different jump process and non-trivial no-jump evolution. Obviously, we can also use $B = \begin{pmatrix} 0 & 0 \\ 0 & 1 \end{pmatrix}$ and $\Gamma = 2/T_\varphi$ for the same master equation (see the brief discussion in Sec. VII of the transformation $B \rightarrow B - b\mathbb{1}$ in the Lindblad equation).

3. Resonator state decay

The decay of a resonator state is usually characterized by the energy decay rate κ , so that in the qubit terminology $\kappa = 1/T_1$. The standard Lindblad form (B1) in this case has $\Gamma = \kappa$ and $B = a$, where a is the annihilation operator, $a|n\rangle = \sqrt{n}|n-1\rangle$. The jump evolution is then

$$|\psi\rangle \rightarrow \frac{a|\psi\rangle}{\text{Norm}}, \quad (\text{B12})$$

with the jump rate [see Eq. (B3)] $\kappa \text{Tr}(a^\dagger a \rho) = \kappa \bar{n}$, where \bar{n} is the average number of photons. The no-jump evolution during time Δt is then

$$\sum_n \alpha_n |n\rangle \rightarrow \frac{\sum_n e^{-n\kappa\Delta t/2} \alpha_n |n\rangle}{\text{Norm}} \approx \frac{\sum_n (1 - n\frac{\kappa}{2}\Delta t) \alpha_n |n\rangle}{\text{Norm}}, \quad (\text{B13})$$

which is similar to the no-jump evolution (B10) for the qubit. Note that the probability of the no-jump evolution is given by the squared norm, $\text{Norm}^2 \approx 1 - \kappa \bar{n} \Delta t$, so that the sum of the jump and no-jump probabilities is 1.

It is interesting to analyze the special case: evolution of a coherent state, $|\lambda\rangle \equiv e^{-|\lambda|^2/2} \sum_n (\lambda^n / \sqrt{n!}) |n\rangle$. Since it is the eigenstate of the operator a , the jump evolution (B12) does not change the state, while the continuous no-jump evolution essentially changes the parameter λ in time, $\lambda(\Delta t) = e^{-\kappa\Delta t/2} \lambda(0)$. Therefore the energy decay is due to the no-jump evolution only. In this (very unusual) case a pure initial state remains pure because

the jump does not change the state and therefore it is essentially a one-scenario (no-jump) evolution.

The standard Lindblad-form evolution for the resonator with $\Gamma = \kappa$ and $B = a$ can be understood in the following way. Let us assume that κ is the coupling with the outside modes, and let us imagine (gedanken-experiment) that we use an ideal photon detector, which clicks every time when a photon escapes from the resonator. When the detector clicks, we know that there is one photon less in the resonator. However, all transitions $|n\rangle \rightarrow |n-1\rangle$ are indistinguishable (because the energy levels are equidistant), and therefore the Bayesian update of the quantum state [49] involves only the rates, which are proportional to n ,

$$\alpha_n |n\rangle \rightarrow \frac{\alpha_n \sqrt{\kappa n} |n-1\rangle}{\text{Norm}}. \quad (\text{B14})$$

It is easy to see that this Bayesian update coincides with the jump process (B12), and therefore the Lindblad-form evolution can be interpreted as being due to an outside measurement with a single-photon detector. [Note that the Lindblad-form master equation describes the ensemble-averaged evolution; this is why we are free to choose any measurement model, in contrast to the case of individual (selective) evolution, which depends on what is actually measured.]

4. Energy relaxation in a 3-level qubit

The energy relaxation (at zero temperature) in a slightly anharmonic superconducting 3-level qubit is sometimes described by essentially the same Lindblad equation as for the resonator, with $\Gamma = 1/T_1$ and $B = a$, so that $B|2\rangle = \sqrt{2}|1\rangle$, $B|1\rangle = |0\rangle$, $B|0\rangle = 0$. This is actually incorrect. The reason is that the qubit is anharmonic, and therefore in the described above gedanken-experiment it is in principle possible to distinguish transitions $|2\rangle \rightarrow |1\rangle$ and $|1\rangle \rightarrow |0\rangle$. Therefore the energy relaxation should be described by two Lindblad terms, with

$$\Gamma_{1 \rightarrow 0} = \frac{1}{T_1}, \quad B_{1 \rightarrow 0} = \begin{pmatrix} 0 & 1 & 0 \\ 0 & 0 & 0 \\ 0 & 0 & 0 \end{pmatrix}, \quad (\text{B15})$$

$$\Gamma_{2 \rightarrow 1} \approx \frac{2}{T_1}, \quad B_{2 \rightarrow 1} = \begin{pmatrix} 0 & 0 & 0 \\ 0 & 0 & 1 \\ 0 & 0 & 0 \end{pmatrix}, \quad (\text{B16})$$

where the top row corresponds to the state $|0\rangle$ and the bottom row corresponds to $|2\rangle$. The formula $\Gamma_{2 \rightarrow 1} \approx 2/T_1$ is not exact because of anharmonicity. If for more accuracy we want to take into account direct transitions $|2\rangle \rightarrow |0\rangle$ (which may become allowed because of anharmonicity), we can introduce the third term in the similar way.

Compared with the two-process description (B15)–(B16), the (incorrect) one-process description (with $B =$

a) adds the extra term $(\sqrt{2}/T_1)\rho_{12}$ into $\dot{\rho}_{01}$, while other terms in these two approaches coincide.

Concluding this Appendix, we emphasize that unraveling of the Lindblad-form evolution into the “jump” and

“no-jump” processes is often useful for gaining intuition in the analysis of decoherence, and it may also be useful in analytical and numerical calculations.

-
- [1] M. A. Nielsen and I. L. Chuang, *Quantum computation and quantum information* (Cambridge University Press, Cambridge, England, 2000).
- [2] J. F. Poyatos, J. I. Cirac, and P. Zoller, *Phys. Rev. Lett.* **78**, 390 (1997).
- [3] I. L. Chuang and M. A. Nielsen, *J. Mod. Opt.* **44**, 2455 (1997).
- [4] D. W. Leung, Ph.D. thesis, Stanford University, 2000; *J. Math. Phys.* **44**, 528, (2003).
- [5] G. M. D’Ariano and P. Lo Presti, *Phys. Rev. Lett.* **86**, 4195 (2001).
- [6] J. B. Altepeter, D. Branning, E. Jeffrey, T. C. Wei, P. G. Kwiat, R. T. Thew, J. L. O’Brien, M. A. Nielsen, and A. G. White, *Phys. Rev. Lett.* **90**, 193601 (2003).
- [7] M. Mohseni and D. A. Lidar, *Phys. Rev. Lett.* **97**, 170501 (2006); M. Mohseni, A. T. Rezakhani, and D. A. Lidar, *Phys. Rev. A* **77**, 032322 (2008).
- [8] A. G. Kofman and A. N. Korotkov, *Phys. Rev. A* **80**, 042103 (2009).
- [9] *New J. Phys.*, focus issue on quantum tomography (2012-2013).
- [10] A. M. Childs, I. L. Chuang, and D. W. Leung, *Phys. Rev. A* **64**, 012314 (2001).
- [11] Y. S. Weinstein, T. F. Havel, J. Emerson, N. Boulant, M. Saraceno, S. Lloyd, and D. G. Cory, *J. Chem. Phys.* **121**, 6117 (2004).
- [12] M. W. Mitchell, C. W. Ellenor, S. Schneider, and A. M. Steinberg, *Phys. Rev. Lett.* **91**, 120402 (2003).
- [13] J. L. O’Brien, G. J. Pryde, A. Gilchrist, D. F. V. James, N. K. Langford, T. C. Ralph, and A. G. White, *Phys. Rev. Lett.* **93**, 080502 (2004).
- [14] M. Riebe, K. Kim, P. Schindler, T. Monz, P. O. Schmidt, T. K. Korber, W. Hansel, H. Haffner, C. F. Roos, and R. Blatt, *Phys. Rev. Lett.* **97**, 220407 (2006).
- [15] D. Hanneke, J. P. Home, J. D. Jost, J. M. Amini, D. Leibfried, and D. J. Wineland, *Nature Phys.* **6**, 13 (2010).
- [16] M. Neeley, M. Ansmann, R. C. Bialczak, M. Hofheinz, N. Katz, E. Lucero, A. O’Connell, H. Wang, A. N. Cleland, and J. M. Martinis, *Nature Phys.* **4**, 523 (2008).
- [17] J. M. Chow, J. M. Gambetta, L. Tornberg, J. Koch, L. S. Bishop, A. A. Houck, B. R. Johnson, L. Frunzio, S. M. Girvin, and R. J. Schoelkopf, *Phys. Rev. Lett.* **102**, 090502 (2009).
- [18] R. C. Bialczak, M. Ansmann, M. Hofheinz, E. Lucero, M. Neeley, A. D. O’Connell, D. Sank, H. Wang, J. Wenner, M. Steffen, A. N. Cleland, and J. M. Martinis, *Nature Phys.* **6**, 409 (2010).
- [19] T. Yamamoto, M. Neeley, E. Lucero, R. C. Bialczak, J. Kelly, M. Lenander, M. Mariantoni, A. D. O’Connell, D. Sank, H. Wang, M. Weides, J. Wenner, Y. Yin, A. N. Cleland, and J. M. Martinis, *Phys. Rev. B* **82**, 184515 (2010).
- [20] J. M. Chow, A. D. Corcoles, J. M. Gambetta, C. Rigetti, B. R. Johnson, J. A. Smolin, J. R. Rozen, G. A. Keefe, M. B. Rothwell, M. B. Ketchen, and M. Steffen, *Phys. Rev. Lett.* **107**, 080502 (2011).
- [21] A. Dewes, F. R. Ong, V. Schmitt, R. Lauro, N. Boulant, P. Bertet, D. Vion, and D. Esteve, *Phys. Rev. Lett.* **108**, 057002 (2012).
- [22] J. Emerson, R. Alicki, and K. Zyczkowski, *J. Opt. B* **7**, S347 (2005).
- [23] C. Dankert, R. Cleve, J. Emerson, and E. Livine, *Phys. Rev. A* **80**, 012304 (2009).
- [24] J. Emerson, M. Silva, O. Moussa, C. Ryan, M. Laforest, J. Baugh, D. G. Cory, and R. Laflamme, *Science*, **317**, 1893 (2007).
- [25] B. Levi, C. C. Lopez, J. Emerson, and D. G. Cory, *Phys. Rev. A* **75**, 022314 (2007).
- [26] A. Bendersky, F. Pastawski, and J. P. Paz, *Phys. Rev. Lett.* **100**, 190403 (2008).
- [27] M. P. da Silva, O. Landon-Cardinal, and D. Poulin, *Phys. Rev. Lett.* **107**, 210404 (2011).
- [28] S. T. Flammia and Y.-K. Liu, *Phys. Rev. Lett.* **106**, 230501 (2011).
- [29] E. Knill, D. Leibfried, R. Reichle, J. Britton, R. B. Blakestad, J. D. Jost, C. Langer, R. Ozeri, S. Seidelin, and D. J. Wineland, *Phys. Rev. A* **77**, 012307 (2008).
- [30] E. Magesan, J. M. Gambetta, and J. Emerson, *Phys. Rev. Lett.* **106**, 180504 (2011).
- [31] E. Magesan, J. M. Gambetta, B. R. Johnson, C. A. Ryan, J. M. Chow, S. T. Merkel, M. P. da Silva, G. A. Keefe, M. B. Rothwell, T. A. Ohki, M. B. Ketchen, and M. Steffen, *Phys. Rev. Lett.* **109**, 080505 (2012).
- [32] A. D. Corcoles, J. M. Gambetta, J. M. Chow, J. A. Smolin, M. Ware, J. Strand, B. L. T. Plourde, and M. Steffen, *Phys. Rev. A* **87**, 030301 (2013).
- [33] J. Kelly, R. Barends, J. Bochmann, B. Campbell, Y. Chen, B. Chiaro, E. Jeffrey, M. Mariantoni, A. Megrant, J. Mutus, C. Neill, P. O’Malley, S. Ohya, P. Roushan, D. Sank, A. Vainsencher, J. Wenner, T. White, A. N. Cleland, and J. M. Martinis, *Bull. Am. Phys. Soc.* **58**, G26.00005 (2013).
- [34] J. M. Chow, J. M. Gambetta, A. D. Corcoles, S. T. Merkel, J. A. Smolin, C. Rigetti, S. Poletto, G. A. Keefe, M. B. Rothwell, J. R. Rozen, M. B. Ketchen, and M. Steffen, *Phys. Rev. Lett.* **109**, 060501 (2012).
- [35] S. T. Flammia, D. Gross, Y.-K. Liu, and J. Eisert, *New J. Phys.* **14**, 095022 (2012).
- [36] A. Shabani, R. L. Kosut, M. Mohseni, H. Rabitz, M. A. Broome, M. P. Almeida, A. Fedrizzi, and A. G. White, *Phys. Rev. Lett.* **106**, 100401 (2011).
- [37] A. Rodionov, A. N. Korotkov, R. L. Kosut, M. Mariantoni, D. Sank, J. Wenner, and J. M. Martinis, *Bull. Am. Phys. Soc.* **58**, G26.00003 (2013).
- [38] N. Boulant, T. F. Havel, M. A. Pravia, and D. G. Cory, *Phys. Rev. A* **67**, 042322 (2003).
- [39] M. M. Wolf, J. Eisert, T. S. Cubitt, and J. I. Cirac, *Phys. Rev. Lett.* **101**, 150402 (2008).
- [40] M. Mohseni, A. T. Rezakhani, and A. Aspuru-Guzik, *Phys. Rev. A* **77**, 042320 (2008); M. Mohseni and A.

- T. Reza khani, Phys. Rev. A **80**, 010101 (2009).
- [41] A. N. Korotkov, “Short notes on $\tilde{\chi}$ -matrix for quantum process tomography” (2010, unpublished).
- [42] To discuss orthogonality and normalization of matrices, we need to define the inner product of matrices A and B of equal size. This can be done by direct generalization of the inner product of two vectors: the matrices are treated as vectors, and the inner product is defined element-by-element as $\langle A|B\rangle \equiv \sum_{i,j} A_{ij}^* B_{ij}$. This is called Frobenius or Hilbert-Schmidt inner product; we use the notation similar to the notation for vectors in quantum mechanics, while in mathematics notations $B : A$ or $\langle B, A\rangle$ are often used. It is easy to see that $\langle A|B\rangle = \sum_{i,j} (A^\dagger)_{ji} B_{ij} = \text{Tr}(A^\dagger B)$. This definition leads to the Frobenius (Hilbert-Schmidt) norm for a matrix: $\|A\| = \sqrt{\text{Tr}(A^\dagger A)} = \sqrt{\sum_{i,j} |A_{ij}|^2}$.
- [43] M. A. Nielsen, Phys. Lett. A **303**, 249 (2002).
- [44] M. Horodecki, P. Horodecki, and R. Horodecki, Phys. Rev. A **60**, 1888 (1999).
- [45] C. C. Lopez, A. Bendersky, J. P. Paz, and D. G. Cory, Phys. Rev. A **81**, 062113 (2010).
- [46] J. Ghosh, A. G. Fowler, and M. R. Geller, Phys. Rev. A **86**, 062318 (2012).
- [47] M. R. Geller and Z. Zhou, Phys. Rev. A **88**, 012314 (2013).
- [48] J. Dalibard, Y. Castin, and K. Mølmer, Phys. Rev. Lett. **68**, 580 (1992).
- [49] A. N. Korotkov, Phys. Rev. B **63**, 115403 (2001); arXiv:1111.4016.
- [50] N. Katz, M. Ansmann, R. C. Bialczak, E. Lucero, R. McDermott, M. Neeley, M. Steffen, E. M. Weig, A. N. Cleland, J. M. Martinis, and A. N. Korotkov, Science **312**, 1498 (2006).
- [51] K. Kraus, *States, effects, and operations: fundamental notions of Quantum Theory* (Springer, Berlin, 1983).
- [52] M. Mariantoni, H. Wang, T. Yamamoto, M. Neeley, R.C. Bialczak, Y. Chen, M. Lenander, E. Lucero, A.D. O’Connell, D. Sank, M. Weides, J. Wenner, Y. Yin, J. Zhao, A.N. Korotkov, A.N. Cleland, and J.M. Martinis, Science **334**, 61 (2011).
- [53] E. Lucero, R. Barends, Y. Chen, J. Kelly, M. Mariantoni, A. Megrant, P. O’Malley, D. Sank, A. Vainsencher, J. Wenner, T. White, Y. Yin, A. N. Cleland and J. M. Martinis, Nature Phys. **8**, 719 (2012).
- [54] A. Galiutdinov, A. N. Korotkov, and J. M. Martinis, Phys. Rev. A **85**, 042321 (2012); J. Ghosh, A. Galiutdinov, Z. Zhou, A. N. Korotkov, J. M. Martinis, and M. R. Geller, Phys. Rev. A **87**, 022309 (2013).
- [55] A. N. Korotkov and K. Keane, Phys. Rev. A **81**, 040103(R) (2010).
- [56] K. Keane and A. N. Korotkov, Phys. Rev. A **86**, 012333 (2012).